

A numerical approximation method for the Fisher-Rao distance between multivariate normal distributions

Frank Nielsen 

Sony Computer Science Laboratories Inc, Tokyo, Japan.

Abstract

We present a simple method to approximate Rao's distance between multivariate normal distributions based on discretizing curves joining normal distributions and approximating Rao's distances between successive nearby normal distributions on the curves by the square root of Jeffreys divergence, the symmetrized Kullback-Leibler divergence. We consider experimentally the linear interpolation curves in the ordinary, natural and expectation parameterizations of the normal distributions, and compare these curves with a curve derived from the Calvo and Oller's isometric embedding of the Fisher-Rao d -variate normal manifold into the cone of $(d+1) \times (d+1)$ symmetric positive-definite matrices [Journal of multivariate analysis 35.2 (1990): 223-242]. We report on our experiments and assess the quality of our approximation technique by comparing the numerical approximations with both lower and upper bounds. Finally, we present several information-geometric properties of the Calvo and Oller's isometric embedding.

Keywords: Fisher-Rao normal manifold; symmetric positive-definite matrix cone; isometric embedding; information geometry

1 Introduction

1.1 The Fisher-Rao normal manifold

Let $\mathbb{P}(d)$ denote the set of symmetric positive-definite matrices, a convex regular cone, and let $\mathcal{N}(d) = \{N(\mu, \Sigma) : (\mu, \Sigma) \in \Lambda(d) = \mathbb{R}^d \times \mathbb{P}(d)\}$ denote the set of d -variate normal distributions, MultiVariate Normals or MVNs for short, also called Gaussian distributions. A MVN distribution $N(\mu, \Sigma)$ has probability density function on the support \mathbb{R}^d :

$$p_{\lambda=(\mu, \Sigma)}(x) = (2\pi)^{\frac{d}{2}} |\Sigma|^{-\frac{1}{2}} \exp\left(-\frac{1}{2}(x - \mu)^\top \Sigma^{-1}(x - \mu)\right), \quad x \in \mathbb{R}^d.$$

The statistical model $\mathcal{N}(d)$ is of dimension $m = \dim(\Lambda(d)) = d + \frac{d(d+1)}{2} = \frac{d(d+3)}{2}$ since it is identifiable, i.e., there is a one-to-one correspondence between $\lambda \in \Lambda(d)$ and $N(\mu, \Sigma) \in \mathcal{N}(d)$ (i.e., $\lambda \leftrightarrow p_\lambda(x)$). The statistical model $\mathcal{N}(d)$ is said regular since the second order derivatives $\frac{\partial^2 p_\lambda}{\partial \lambda_i \partial \lambda_j}$ and third order derivatives $\frac{\partial^3 p_\lambda}{\partial \lambda_i \partial \lambda_j \partial \lambda_k}$ are smooth functions (defining the metric and cubic tensors in information geometry [4]), and the set of first order partial derivatives $\{\frac{\partial p_\lambda}{\partial \lambda_1}, \dots, \frac{\partial p_\lambda}{\partial \lambda_1}\}$ are linearly independent.

Let $\text{Cov}(X)$ denote the covariance of X or variance when X is scalar. The Fisher information matrix (FIM) is the symmetric semi-positive definite matrix:

$$I(\lambda) = \text{Cov}[\nabla \log p_\lambda(x)] \succeq 0.$$

For regular statistical models $\{p_\lambda\}$, the FIM is positive-definite: $I(\lambda) \gg 0$.

Remark 1 *An example of non-regular statistical model is the set $\mathcal{D} = \{\delta_\theta(x) : \theta \in \mathbb{R}\}$ of Dirac distributions where $\delta_\theta(x) = \begin{cases} 1, & x = \theta, \\ 0, & x \neq \theta \end{cases}$. Indeed, we have the following FIM of a Dirac distribution δ_θ : $I(\theta) = \text{Var}[\delta_\theta] = E[X^2] - E[X]^2 = 0$. The family of Dirac distributions is an example of non-regular model where the support of the distributions depends on the model parameter (i.e., $\text{supp}(\delta_\theta) = \theta$). Mathematical statistics of non-regular models are considered in [2].*

The FIM is covariant under reparameterization of the statistical model. That is, $\theta(\lambda)$ be a new parameterization of the MVNs. Then we have

$$I_\theta(\lambda) = \left(\frac{\partial \lambda}{\partial \theta} \right)^\top I_\lambda(\lambda(\theta)) \left(\frac{\partial \lambda}{\partial \theta} \right).$$

For example, we may parameterize univariate normal distributions by $\lambda = (\mu, \sigma^2)$ or $\theta = (\mu, \sigma)$. We obtain the following Fisher information matrices for these parameterizations:

$$I_\lambda(\lambda(\mu, \sigma)) = \begin{bmatrix} \frac{1}{\sigma^2} & 0 \\ 0 & \frac{1}{2\sigma^4} \end{bmatrix}, \quad I_\theta(\theta(\mu, \sigma)) = \begin{bmatrix} \frac{1}{\sigma^2} & 0 \\ 0 & \frac{1}{2\sigma^2} \end{bmatrix}.$$

In higher dimensions, parameterization λ corresponds to the parameterization (μ, Σ) while parameterization $\theta = (\mu, L)$ where $\Sigma = LL^\top$ is the unique Cholesky decomposition with $L \in \text{GL}(d)$, the group of invertible $d \times d$ matrices. Another useful parameterization for optimization is the log-Cholesky parameterization [52] ($\eta = (\mu, \log \sigma^2) \in \mathbb{R}^2$ for univariate normals) which ensures that gradient descent stay in the domain. The Fisher information matrix with respect to the log-Cholesky parameterization is $I_\eta(\eta(\mu, \sigma)) = \begin{bmatrix} \frac{1}{\sigma^2} & 0 \\ 0 & 2 \end{bmatrix}$ with $\eta(\mu, \sigma) \in \mathbb{R}^2$.

Since the statistical model $\mathcal{N}(d)$ is identifiable and regular, the Fisher information matrix can be written equivalently using the first two Bartlett identities as

$$I(\mu, \Sigma) = \text{Cov}[\nabla \log p_{(\mu, \Sigma)}] = E \left[\nabla \log p_{(\mu, \Sigma)} \nabla \log p_{(\mu, \Sigma)}^\top \right], \quad (1)$$

$$= -E \left[\nabla^2 \log p_{(\mu, \Sigma)} \right]. \quad (2)$$

For multivariate distributions parameterized by a m -dimensional vector

$$\theta = (\theta_1, \dots, \theta_d, \theta_{d+1}, \dots, \theta_m) \in \mathbb{R}^m,$$

with $\mu = (\theta_1, \dots, \theta_d)$ and $\Sigma(\theta) = \text{vech}(\theta_{d+1}, \dots, \theta_m)$ (inverse half-vectorization of matrices), we have [83, 55, 41]:

$$I(\theta) = [I_{ij}(\theta)], \quad I_{ij}(\theta) = \left(\frac{\partial \mu}{\partial \theta_i} \right)^\top \Sigma^{-1} \frac{\partial \mu}{\partial \theta_j} + \frac{1}{2} \text{tr} \left(\Sigma^{-1} \frac{\partial \mu}{\partial \theta_i} \Sigma^{-1} \frac{\partial \mu}{\partial \theta_j} \right).$$

By equipping the regular statistical model $\mathcal{N}(d)$ with the Fisher information metric

$$g_{\mathcal{N}}^{\text{Fisher}}(\mu, \Sigma) = \text{Cov}[\nabla \log p_{(\mu, \Sigma)}(x)]$$

we get a Riemannian manifold $\mathcal{M} = \mathcal{M}_{\mathcal{N}}$ called the Fisher-Rao Gaussian [83]. The induced Riemannian geodesic distance $\rho_{\mathcal{N}}(\cdot, \cdot)$ is called the Rao distance [6] or the Fisher-Rao distance [78, 62, 20]:

$$\rho_{\mathcal{N}}(N(\lambda_1), N(\lambda_2)) = \inf_c \{\text{Length}(c) : c(0) = p_{\lambda_1}, c(1) = p_{\lambda_2}\},$$

where the Riemannian length of a smooth curve $c(t)$ is defined by

$$\text{Length}(c) = \int_0^1 \underbrace{\sqrt{\langle \dot{c}(t), \dot{c}(t) \rangle_{c(t)}}}_{ds_{\mathcal{N}}(t)} dt.$$

The minimizing curve $\gamma_{\mathcal{N}}(p_{\lambda_1}, p_{\lambda_2}; t)$ is called the Fisher geodesic: It is also an auto-parallel curve for the Levi-Civita connection ∇^{Fisher} induced by the Fisher metric g^{Fisher} . See [4] for details.

Remark 2 *If we consider the Riemannian manifold $(\mathcal{M}, \beta g)$ for $\beta > 0$ then the length element is scaled by $\sqrt{\beta}$: $ds_{\beta g} = \beta ds_g$. It follows that the length of a curve c is $\text{Length}_{\beta g}(c) = \sqrt{\beta} \text{Length}_g(c)$. However, the geodesics are the same: $\gamma_{\beta g}(p_1, p_2; t) = \gamma_g(p_1, p_2; t)$ with $\gamma_g(p_1, p_2; 0) = p_1$ and $\gamma_g(p_1, p_2; 1) = p_2$.*

Historically, Hotelling [42] first used this Fisher Riemannian geodesic distance in the late 1920's. From the viewpoint of information geometry [4], the Fisher metric is the unique Markov invariant metric up to rescaling [17, 8, 34] and the Fisher-Rao distance has been used to design statistical hypothesis testing [12, 14, 79, 73], to measure the distance between the prior and posterior distributions in Bayesian statistics [38], clustering [86, 48], in signal processing [80, 49, 39, 23], and in deep learning [51] among others.

The squared line element

$$ds_{\mathcal{N}}^2(\mu, \Sigma) = g_{(\mu, \Sigma)}((d\mu, d\Sigma), (d\mu, d\Sigma)) = \begin{bmatrix} d\mu \\ d\Sigma \end{bmatrix}^{\top} I(\mu, \Sigma) \begin{bmatrix} d\mu \\ d\Sigma \end{bmatrix}$$

induced by the Fisher information metric of the normal family is

$$ds_{\mathcal{N}}^2(\mu, \Sigma) = d\mu^{\top} \Sigma^{-1} d\mu + \frac{1}{2} \text{tr} \left((\Sigma^{-1} d\Sigma)^2 \right). \quad (3)$$

Remark 3 *The family $\mathcal{N}(d)$ of normal distributions forms an exponential family [96]:*

$$\mathcal{N}(d) = \left\{ p_{\theta(\lambda)} = \exp \left(\langle \theta_v(\mu), x \rangle + \langle \theta_M(\Sigma), xx^{\top} \rangle - F_{\mathcal{N}}(\theta_v, \theta_M) \right) \right\},$$

with $\theta(\lambda) = (\theta_v = (\Sigma^{-1} \mu, \theta_M = \frac{1}{2} \Sigma^{-1}))$ the natural parameters and log-partition/cumulant function

$$F_{\mathcal{N}}(\theta) = \frac{1}{2} \left(d \log \pi - \log |\theta_M| + \frac{1}{2} \theta_v^{\top} \theta_M^{-1} \theta_v \right).$$

The matrix inner product is $\langle M_1, M_2 \rangle = \text{tr}(M_1 M_2^{\top})$. Using Eq. 2, it follows that the MVN FIM is $I_{\theta}(\theta) = -E[\nabla^2 \log p_{\theta}] = \nabla^2 F(\theta)$. As an exponential family [4], we also have $I_{\theta}(\theta) = E[t(x)]$, where

$t(x) = (x, xx^\top)$ is the sufficient statistic. Thus the Fisher metric is a Hessian metric [81]. Let $F_{\mathcal{N}}(\theta_v, \theta_M) = F_v(\theta_v) + F_M(\theta_M)$ with $F_v(\theta_v) = \frac{1}{2} (d \log \pi + \frac{1}{2} \theta_v^\top \theta_M^{-1} \theta_v)$ and $F_M(\theta_M) = -\frac{1}{2} \log |\theta_M|$. We have

$$I(\theta(\lambda)) = \nabla^2 F_{\mathcal{N}}(\theta(\mu, \Sigma)) = \begin{bmatrix} \Sigma^{-1} & 0 \\ 0 & \frac{1}{2} \nabla_{\theta_M}^2 \log |\frac{1}{2} \Sigma^{-1}| \end{bmatrix}.$$

Therefore $ds_{\mathcal{N}}^2(\mu, \Sigma) = ds_v^2 + ds_M^2$ with $ds_v^2(\mu) = d\mu^\top \Sigma^{-1} d\mu$ and $ds_M^2(\Sigma) = \frac{1}{2} \text{tr} \left((\Sigma^{-1} d\Sigma)^2 \right)$. Let us note in passing that $\nabla_{\theta_M}^2 \log |\theta_M|$ is a fourth order tensor [84].

The family $\mathcal{N}(d)$ can also be considered as an elliptical family [15], thus highlighting the affine-invariance property of the Fisher information metric. That is, the Fisher metric is invariant with respect to affine transformations [11]: Let (a, A) be an element of the affine group $\text{Aff}(d)$ with $a \in \mathbb{R}^d$ and $A \in \text{GL}(d)$. The group identity element is $e = (0, I)$ and the group operations are $(a_1, A_1) \cdot (a_2, A_2) = (a_1 + A_1 a_2, A_1 A_2)$ and $(a, A)^{-1} = (-A^{-1} a, A^{-1})$. Then we have

Property 1 (Fisher-Rao affine-invariance) For all $A \in \text{GL}(d), a \in \mathbb{R}^d$, we have $\rho_{\mathcal{N}}(N(A\mu_1 + a, A\Sigma_1 A^\top), N(A\mu_2 + a, A\Sigma_2 A^\top)) = \rho_{\mathcal{N}}(N(\mu_1, \Sigma_1), N(\mu_2, \Sigma_2))$.

It follows that we have

$$\begin{aligned} \rho_{\mathcal{N}}(N(\mu_1, \Sigma_1), N(\mu_2, \Sigma_2)) &= \rho_{\mathcal{N}}(N_{\text{std}}, N(\Sigma_1^{-\frac{1}{2}}(\mu_2 - \mu_1), \Sigma_1^{-\frac{1}{2}} \Sigma_2 \Sigma_1^{-\frac{1}{2}})), \\ &= \rho_{\mathcal{N}}(N(\Sigma_2^{-\frac{1}{2}}(\mu_1 - \mu_2), \Sigma_2^{-\frac{1}{2}} \Sigma_1 \Sigma_2^{-\frac{1}{2}}), N_{\text{std}}), \end{aligned}$$

where $N_{\text{std}} = N(0, I)$ is the standard d -variate distribution. The family of normal distributions can be obtained from the standard normal distribution by the action of the affine group $\text{Aff}(d)$:

$$N(\mu, \Sigma) = (\mu, \Sigma^{\frac{1}{2}}) \cdot N_{\text{std}} = N((\mu, \Sigma^{\frac{1}{2}}) \cdot (0, I)).$$

1.2 Fisher-Rao distance between normal distributions

In general, the Fisher-Rao distance $\rho_{\mathcal{N}}(N_1, N_2)$ between two multivariate normal distributions N_1 and N_2 is not known in closed-form [29, 9, 44, 45], and several lower and upper bounds [87], and numerical techniques like costly and numerically instable geodesic shooting [40, 75, 7] have been investigated. See [76] for a recent review.

Two difficulties to calculate the Fisher-Rao distance are

- to know explicitly the expression of the Riemannian Fisher-Rao geodesic $\gamma_{\mathcal{N}}^{\text{FR}}$ and
- to integrate in closed-form the length element $ds_{\mathcal{N}}$ along this Riemannian geodesic.

Note that the Fisher-Rao geodesics [4] $\gamma_{\mathcal{N}}^{\text{FR}}(t)$ are parameterized by constant speed (i.e., $\dot{\mu}(t) = \dot{\mu}(0)$ and $\dot{\Sigma}(t) = \dot{\Sigma}(0)$, proportional to arc length parameterization). However, in several special cases, the Fisher-Rao distance between normal distributions belonging to restricted subsets of \mathcal{N} is known.

Three such prominent cases are

- when the normal distributions are univariate ($d = 1$),

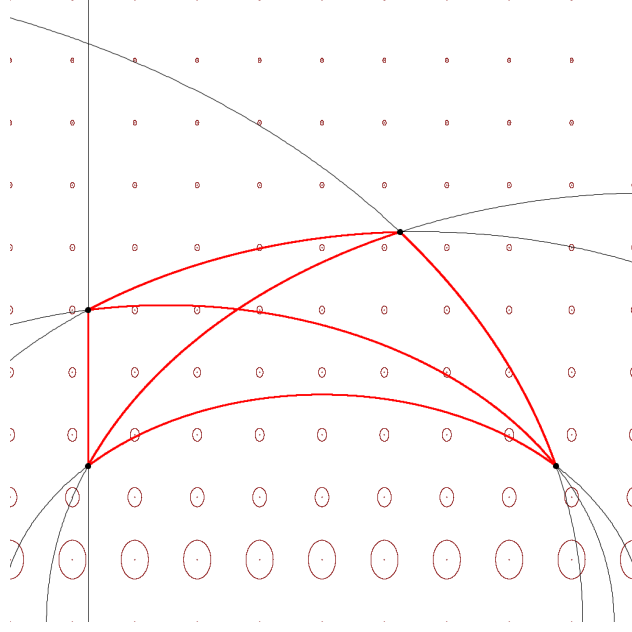


Figure 1: Four univariate normal distributions $N_1 = N(0, 1)$, $N_2 = N(3, 1)$, $N_3 = N(2, 2.5)$, $N_4 = N(0, 2)$, and their pairwise full geodesics and geodesics linking them. The Fisher-Rao distances are $\rho_{\mathcal{N}}(N_1, N_2) = 2.6124\dots$, $\rho_{\mathcal{N}}(N_3, N_4) = 0.9317\dots$, $\rho_{\mathcal{N}}(N_1, N_4) = 0.9803\dots$, $\rho_{\mathcal{N}}(N_2, N_3) = 1.4225\dots$, $\rho_{\mathcal{N}}(N_2, N_4) = 2.1362\dots$, and $\rho_{\mathcal{N}}(N_1, N_3) = 1.7334\dots$

- when we consider the set $\mathcal{N}_\mu = \{N(\mu, \Sigma) : \Sigma \in \mathcal{P}(d)\} \subset \mathcal{M}_{\mathcal{N}}$ of normal distributions share the same mean μ (with the embedded submanifold $\mathcal{S}_\mu \in \mathcal{M}$), and
- when we consider the set $\mathcal{N}_\Sigma = \{N(\mu, \Sigma) : \Sigma \in \mathcal{P}(d)\} \subset \mathcal{N}$ of normal distributions share the same covariance matrix Σ (with the corresponding embedded submanifold $\mathcal{S}_\Sigma \in \mathcal{M}$)

Let us report the formula of the Fisher-Rao distance in these three cases:

- In the univariate case $\mathcal{N}(1)$, the Fisher-Rao distance between $N_1 = N(\mu_1, \sigma_1^2)$ and $N_2 = N(\mu_2, \sigma_2^2)$ can be derived from the hyperbolic distance expressed in the Poincaré upper space:

$$\rho_{\mathcal{N}}(N(\mu_1, \sigma_1^2), N(\mu_2, \sigma_2^2)) = \sqrt{2} \log \left(\frac{1 + \Delta(\mu_1, \sigma_1; \mu_2, \sigma_2)}{1 - \Delta(\mu_1, \sigma_1; \mu_2, \sigma_2)} \right), \quad (4)$$

with

$$\Delta(a, b; c, d) = \sqrt{\frac{(c - a)^2 + 2(d - b)^2}{(c - a)^2 + 2(d + b)^2}}. \quad (5)$$

Figure 1 displays four univariate normal distributions with their pairwise geodesics and Fisher-Rao distances.

- In the second case, the Rao distance between $N_1 = N(\mu, \Sigma_1)$ and $N_2 = N(\mu, \Sigma_2)$ has been

reported in [82, 46, 83, 94]:

$$\rho_{\mathcal{N}_\mu}(N_1, N_2) = \sqrt{\frac{1}{2} \sum_{i=1}^d \log^2 \lambda_i(\Sigma_1^{-1} \Sigma_2)}, \quad (6)$$

$$= \rho_{\mathcal{P}}(\Sigma_1, \Sigma_2), \quad (7)$$

where $\lambda_i(M)$ denotes the i -th largest eigenvalue of matrix M . Let us notice that $\rho_{\mathcal{N}_\mu}((\mu, \Sigma_1), (\mu, \Sigma_2)) = \rho_{\mathcal{N}_\mu}((\mu, \Sigma_1^{-1}), (\mu, \Sigma_2^{-1}))$ since $\lambda_i(\Sigma_2^{-1} \Sigma_1) = \frac{1}{\lambda_i(\Sigma_1^{-1} \Sigma_2)}$ and $\log^2 \lambda_i(\Sigma_2^{-1} \Sigma_1) = (-\log \lambda_i(\Sigma_1^{-1} \Sigma_2))^2 = \log^2 \lambda_i(\Sigma_1^{-1} \Sigma_2)$. Also, matrix $\Sigma_1^{-1} \Sigma_2$ may not be SPD: We may consider the SPD matrix $\Sigma_1^{-\frac{1}{2}} \Sigma_2 \Sigma_1^{-\frac{1}{2}}$ which is SPD and such that $\lambda_i(\Sigma_1^{-1} \Sigma_2) = \lambda_i(\Sigma_1^{-\frac{1}{2}} \Sigma_2 \Sigma_1^{-\frac{1}{2}})$. The Rao distance of Eq. 7 can be equivalently written [16] as

$$\rho_{\mathcal{N}_\mu}(N_1, N_2) = \frac{1}{\sqrt{2}} \left\| \log \left(\Sigma_1^{-\frac{1}{2}} \Sigma_2 \Sigma_1^{-\frac{1}{2}} \right) \right\|.$$

This metric distance was rediscovered and analyzed in [32]. Let $\rho_{\text{SPD}}(P_1, P_2) = \sqrt{\sum_{i=1}^d \log^2 \lambda_i(P_1^{-1} P_2)}$ so that $\rho_{\mathcal{N}_\mu}(N(\mu, P_1), N(\mu, P_2)) = \frac{1}{\sqrt{2}} \rho_{\text{SPD}}(P_1, P_2)$.

This Riemannian SPD distance ρ_{SPD} enjoys the following invariance properties:

- Invariance by congruence transformation:

$$\forall X \in \text{GL}(d), \rho_{\text{SPD}}(X P_1 X^\top, X P_2 X^\top) = \rho_{\text{SPD}}(P_1, P_2), \quad (8)$$

- Invariance by inversion:

$$\forall P_1, P_2 \in \mathbb{P}(d), \rho(P_1^{-1}, P_2^{-1}) = \rho_{\text{SPD}}(P_1, P_2).$$

Let $P_1 = L_1 L_1^\top$ be the unique Cholesky decomposition. Then apply the congruence invariance for $X = L_1^{-1}$:

$$\rho_{\text{SPD}}(P_1, P_2) = \rho_{\text{SPD}}(L_1^{-1} P_1 (L_1^{-1})^\top, L_1^{-1} P_2 (L_1^{-1})^\top) = \rho_{\text{SPD}}(I, L_1^{-1} P_2 (L_1^{-1})^\top). \quad (9)$$

We can also consider the factorization $P_1 = S_1 S_1$ where $S_1 = P_1^{\frac{1}{2}}$ is the unique symmetric square root matrix. Then we have

$$\rho_{\text{SPD}}(P_1, P_2) = \rho_{\text{SPD}}(S_1^{-1} P_1 (S_1^{-1})^\top, S_1^{-1} P_2 (S_1^{-1})^\top) = \rho_{\text{SPD}}(I, S_1^{-1} P_2 (S_1^{-1})^\top).$$

Remark 4 *In practice the covariance matrices usually need to be estimated from samples (sample covariance matrices) before measuring the distances between them. In large dimensions, these approximations suffer severe errors and better consistent estimates of statistical distances based on random matrix theory (RMT) have been proposed in [89].*

- The Rao distance between $N_1 = N(\mu_1, \Sigma)$ and $N_2 = N(\mu_2, \Sigma)$ has been reported in closed-form [76] (Proposition 3). Their method is detailed in the Appendix A. We consider the following simple scheme based on the inverse $\Sigma^{-\frac{1}{2}}$ of the symmetric square root factorization of $\Sigma = \Sigma^{\frac{1}{2}} \Sigma^{\frac{1}{2}}$ (and $(\Sigma^{-\frac{1}{2}})^\top = \Sigma^{-\frac{1}{2}}$). Let us use the affine invariance

property of the Fisher-Rao distance under the transformation $\Sigma^{-\frac{1}{2}}$ and then apply affine invariance under translation:

$$\begin{aligned}\rho_{\mathcal{N}}(N(\mu_1, \Sigma), N(\mu_2, \Sigma)) &= \rho_{\mathcal{N}}(N(\Sigma^{-\frac{1}{2}}\mu_1, \Sigma^{-\frac{1}{2}}\Sigma\Sigma^{-\frac{1}{2}}), N(\Sigma^{-\frac{1}{2}}\mu_2, \Sigma^{-\frac{1}{2}}\Sigma\Sigma^{-\frac{1}{2}})), \\ &= \rho_{\mathcal{N}}(N(0, I), N(\Sigma^{-\frac{1}{2}}(\mu_2 - \mu_1), I)), \\ &= \rho_{\mathcal{N}}(N(0, 1), N(\|\Sigma^{-\frac{1}{2}}(\mu_2 - \mu_1)\|_2, 1)).\end{aligned}$$

The right-hand side Fisher-Rao distance is computed from Eq. 4 and justified by the method [76] (Proposition 3) described in the Appendix A. Section 1.5 shall report a simpler closed-form formula by proving that the Fisher-Rao distance between $N(\mu_1, \Sigma)$ and $N(\mu_2, \Sigma)$ is a scalar function of their Mahalanobis distance [54] using an algebraic method.

1.3 Fisher-Rao distance: Totally vs non-totally geodesic submanifolds

Consider $\mathcal{N}' = \{N(\lambda) : \lambda \in \Lambda'\} \subset \mathcal{N}$ a statistical submodel of the MVN statistical model \mathcal{N} . Using the Fisher information matrix $I_{\lambda'}(\lambda')$, we get the intrinsic Fisher-Rao manifold $\mathcal{M}' = \mathcal{M}_{\mathcal{N}'}$. We may also consider \mathcal{M}' to be an embedded submanifold of \mathcal{M} . Let us write $\mathcal{S}' = \mathcal{S}_{\mathcal{N}'} \subset \mathcal{M}$ the embedded submanifold.

A totally geodesic submanifold $\mathcal{S}' \subset \mathcal{M}$ is such that the geodesics $\gamma_{\mathcal{M}'}(N'_1, N'_2; t)$ fully stay in \mathcal{M}' for any pair of points $N'_1, N'_2 \in \mathcal{N}'$. For example, the submanifold $\mathcal{M}_\mu = \{N(\mu, \Sigma) : \Sigma \in \mathbb{P}(d)\} \subset \mathcal{M}$ of MVNs with fixed mean μ is a totally geodesic submanifold [36] of \mathcal{M} but the submanifold $\mathcal{M}_\Sigma = \{N(\mu, \Sigma) : \mu \in \mathbb{R}^d\} \subset \mathcal{M}$ of MVNs sharing the same covariance matrix Σ is not totally geodesic. When an embedded submanifold $\mathcal{S} \subset \mathcal{M}$ is totally geodesic, we always have $\rho_{\mathcal{M}}(N_1, N_2) = \rho_{\mathcal{S}}(N_1, N_2)$. Thus we have $\rho_{\mathcal{N}}(N(\mu, \Sigma_1), N(\mu, \Sigma_2)) = \rho_{\text{SPD}}(\Sigma_1, \Sigma_2)$. However, when an embedded submanifold $\mathcal{S} \subset \mathcal{M}$ is not totally geodesic, we have $\rho_{\mathcal{M}}(N_1, N_2) \leq \rho_{\mathcal{S}}(N_1, N_2)$ because the Riemannian geodesic length in \mathcal{S} is necessarily longer or equal than the Riemannian geodesic length in \mathcal{M} . The merit to consider submanifolds is to be able to calculate in closed form the Fisher-Rao distance which may then provide an upper bound on the Fisher-Rao distance for the full statistical model. For example, consider $N_1 = N(\mu_1, \Sigma)$ and $N_2 = N(\mu_2, \Sigma)$ in \mathcal{M}_Σ , a non-totally geodesic submanifold. The Rao distance between N_1 and N_2 in \mathcal{M} is upper bounded by the Riemannian distance in \mathcal{M}_Σ (with line element $ds_{\Sigma}^2 = d\mu^\top \Sigma^{-1} d\mu$) which corresponds to the Mahalanobis distance [54, 6] $\Delta_\Sigma(\mu_1, \mu_2)$:

$$\rho_{\mathcal{M}_\Sigma}(N_1, N_2) \leq \Delta_\Sigma(\mu_1, \mu_2) := \sqrt{(\mu_2 - \mu_1)^\top \Sigma^{-1} (\mu_2 - \mu_1)}. \quad (10)$$

The Mahalanobis distance can be interpreted as the Euclidean distance $D_E(p, q) = \Delta_I(p, q) = \sqrt{(p - q)^\top (p - q)}$ (where I denotes the identity matrix) after an affine transformation: Let $\Sigma = LL^\top = U^\top U$ be the Cholesky decomposition of $\Sigma \gg 0$ with L a lower triangular matrix or $U = L^\top$ an upper triangular matrix. Then we have

$$\begin{aligned}\Delta_\Sigma(\mu_1, \mu_2) &= \sqrt{(\mu_2 - \mu_1)^\top (L^\top)^{-1} L^{-1} (\mu_2 - \mu_1)}, \\ &= \|\Sigma^{-\frac{1}{2}}(\mu_2 - \mu_1)\|_2, \\ &= \Delta_I(L^{-1}\mu_1, L^{-1}\mu_2) = D_E(L^{-1}\mu_1, L^{-1}\mu_2),\end{aligned}$$

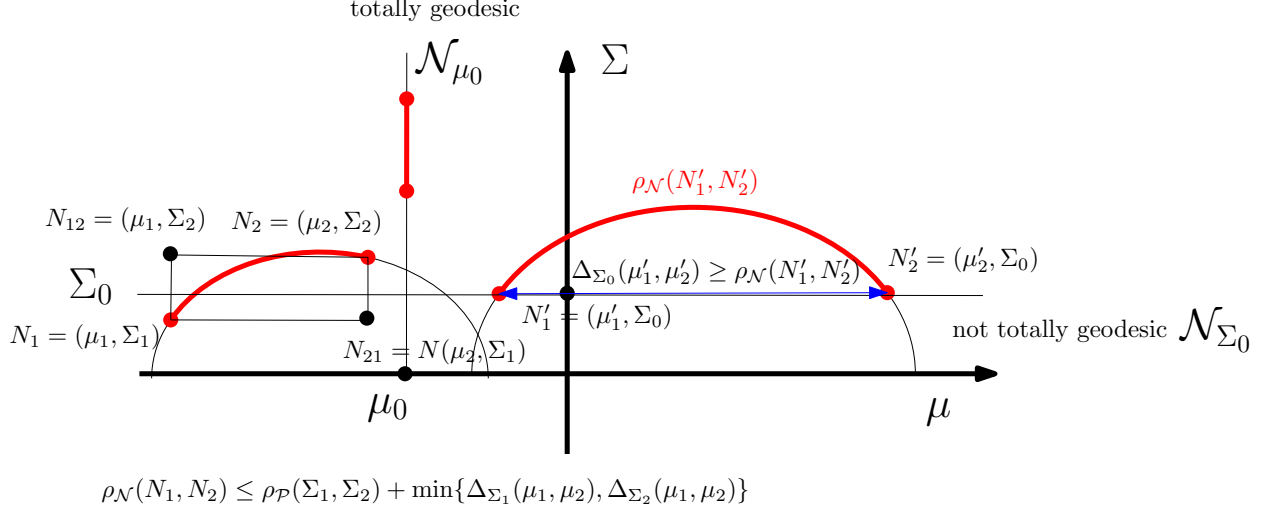


Figure 2: The submanifolds \mathcal{N}_Σ are not totally geodesic (i.e., $\rho_{\mathcal{N}'}(N'_1, N'_2)$ is upper bounded by their Mahalanobis distance) but the submanifolds \mathcal{N}_μ are totally geodesic. Using the triangle inequality of the Riemannian metric distance $\rho_{\mathcal{N}'}$, we can upper bound $\rho_{\mathcal{N}'}(N_1, N_2)$.

where $\|\cdot\|_2$ denotes the vector ℓ_2 -norm.

The Rao distance ρ_Σ of Eq. 25 between two MVNs with fixed covariance matrix emanates from the property that the submanifold $\mathcal{M}_{[v],\Sigma} = \{N(av, \Sigma) : a \in \mathbb{R}\}$ is totally geodesic [85].

Let us emphasize that for a submanifold $\mathcal{S} \subset \mathcal{M}$ to be totally geodesic or not depend on the underlying metric in \mathcal{M} . A same subset $\mathcal{N}' \subset \mathcal{N}$ with \mathcal{N} equipped with two different metric g_1 and g_2 can be totally geodesic wrt. g_1 and non-totally geodesic wrt. g_2 . See Remark 6 for such an example.

In general, using the triangle inequality of the Riemannian metric distance $\rho_{\mathcal{N}'}$, we can upper bound $\rho_{\mathcal{N}'}(N_1, N_2)$ with $N_1 = (\mu_1, \Sigma_1)$ and $N_2 = (\mu_2, \Sigma_2)$ as follows:

$$\begin{aligned} \rho_{\mathcal{N}'}(N_1, N_2) &\leq \rho_{\mathcal{M}_{\mu_1}}(N_1, N_{12}) + \rho_{\mathcal{M}_{\Sigma_2}}(N_{12}, N_2), \\ &\leq \rho_{\mathcal{M}_{\Sigma_1}}(N_1, N_{21}) + \rho_{\mathcal{M}_{\mu_2}}(N_{21}, N_2), \end{aligned}$$

where $N_{12} = (\mu_1, \Sigma_2)$ and $N_{21} = N(\mu_2, \Sigma_1)$. See Figure 2 for an illustration. Furthermore, since $\rho_{\mathcal{N}_{\Sigma_1}}(N_1, N_{21}) \leq \Delta_{\Sigma_1}(\mu_1, \mu_2)$ and $\rho_{\mathcal{N}_{\Sigma_2}}(N_{12}, N_2) \leq \Delta_{\Sigma_2}(\mu_1, \mu_2)$, we get the following upper bound on the Rao distance between MVNs:

$$\rho_{\mathcal{N}'}(N_1, N_2) \leq \rho_{\mathcal{P}}(\Sigma_1, \Sigma_2) + \min\{\Delta_{\Sigma_1}(\mu_1, \mu_2), \Delta_{\Sigma_2}(\mu_1, \mu_2)\}. \quad (11)$$

See also [19].

In general, the difficulty of calculating the Fisher-Rao distance comes from the fact that

1. we do not know the Fisher-Rao geodesics with boundary value conditions (BVP) in closed form (only the geodesics with initial value conditions [16], IVP, are partially known),
2. we have to integrate the line element $ds_{\mathcal{N}'}$ along the geodesic.

As we shall see in §3.1, the above first problem is much hard to solve than the second problem which can be easily approximated by discretizing the curve. The lack of a closed-form formula

and fast and good approximations for $\rho_{\mathcal{N}}$ between MVNs is a current limiting factor for its use in applications. Indeed, many applications (e.g., [21, 61]) consider the restricted case of the Rao distance between zero-centered MVNs which have closed-form (distance of Eq. 7 in the SPD cone). The SPD cone is a symmetric Hadamard manifold and its isometries have been fully studied and classified in [26] (§4). The Fisher-Rao geometry of zero-centered generalized MVNs was recently studied in [91].

1.4 Contributions and paper outline

The main contribution of this paper is to propose an approximation of $\rho_{\mathcal{N}}$ based on Calvo & Oller’s embedding [14] (C&O for short) and report its experimental performance. First, we concisely recall C&O’s family of embeddings f_{β} of $\mathcal{N}(d)$ as submanifolds $\overline{\mathcal{N}}_{\beta}$ of $\mathcal{P}(d+1)$ in Section 2. Next, we present our approximation technique in Section 3 which differs from the usual geodesic shooting approach [40], and report experimental results. Finally, we study some information-geometric properties [4] of the isometric embedding in §5 like the fact that it preserves mixture geodesics (embedded C&O submanifold is autoparallel with respect to the mixture affine connection) but not exponential geodesics. Besides, we prove that the Fisher-Rao distance between multivariate normal distributions sharing the same covariance matrix is a scalar function of their Mahalanobis distance in §1.5 using the framework of Eaton [28] of maximal invariants.

1.5 A closed-form formula for the Fisher-Rao distance between normal distributions sharing the same covariance matrix

Consider the Fisher-Rao distance between $N_1 = (\mu_1, \Sigma)$ and $N_2 = (\mu_2, \Sigma)$ for a fixed covariance matrix Σ and the translation action $a \cdot \mu := \mu + a$ of the translation group \mathbb{R}^d (a subgroup of the affine group). Both the Fisher-Rao distance and the Mahalanobis distance are invariant under translations:

$$\rho_{\mathcal{N}}((\mu_1 + a, \Sigma), (\mu_2 + a, \Sigma)) = \rho_{\mathcal{N}}((\mu_1, \Sigma), (\mu_2, \Sigma)), \quad \Delta_{\Sigma}(\mu_1 + a, \mu_2 + a) = \Delta_{\Sigma}(\mu_1, \mu_2).$$

To prove that $\rho_{\mathcal{N}}((\mu_1, \Sigma), (\mu_2, \Sigma)) = h_{\text{FR}}(\Delta_{\Sigma}(\mu_1, \mu_2))$ for a scalar function h_{FR} , we shall prove that the Mahalanobis distance is a maximal invariant and use the framework of maximal invariants of Eaton [28] (Chapter 2) who proved that any other invariant function is necessarily a function of a maximal invariant, i.e., a function of the Mahalanobis distance. The Mahalanobis distance is maximal invariant because when $\Delta_{\Sigma}(\mu_1, \mu_2) = \Delta_{\Sigma}(\mu'_1, \mu'_2)$ there exists $a \in \mathbb{R}^d$ such that $(\mu_1 + a, \mu_2 + a) = (\mu'_1, \mu'_2)$: Indeed, we may consider the Cholesky decomposition $\Sigma = LL^{\top}$ so that $\Delta_{\Sigma}(\mu_1, \mu_2) = \Delta_I(L^{\top}\mu_1, L^{\top}\mu_2)$. Let $m_1 = L^{\top}\mu_1$, $m_2 = L^{\top}\mu_2$, $m'_1 = L^{\top}\mu'_1$ and $m'_2 = L^{\top}\mu'_2$. We have to prove equivalently that when $\|m_1 - m_2\|_2 = \|m'_1 - m'_2\|_2$ that there exists $a \in \mathbb{R}^d$ such that $(m_1 + a, m_2 + a) = (m'_1, m'_2)$. It suffices to let $a = m'_1 - m_1$ and consider $m_1 - m_2 = m'_1 - m'_2$. Then we have $m_2 + a = m_2 + m'_1 - m_1 = m'_2 - m'_1 + m'_1 = m'_2$. Thus using Eaton’s theorem [28], there exists a scalar function h_{FR} such that $\rho_{\mathcal{N}}((\mu_1, \Sigma), (\mu_2, \Sigma)) = h_{\text{FR}}(\Delta_{\Sigma}(\mu_1, \mu_2))$.

To find explicitly the scalar function $h_{\text{FR}}(\cdot)$, let us consider the univariate case of normal distributions for which the Fisher-Rao distance is given in closed form in Eq. 4. In that case, the univariate Mahalanobis distance is $\Delta_{\sigma^2}(\mu_1, \mu_2) = \sqrt{(\mu_2 - \mu_1)(\sigma^2) - 1(\mu_2 - \mu_1)} = \frac{|\mu_2 - \mu_1|}{\sigma}$ and we

can write formula of Eq. 4 as $h_{\text{FR}}(\Delta_{\sigma^2}(\mu_1, \mu_2))$ with

$$h_{\text{FR}}(u) = \sqrt{2} \log \left(\frac{\sqrt{8+u^2}+u}{\sqrt{8+u^2}-u} \right), \quad (12)$$

$$= \sqrt{2} \operatorname{arccosh} \left(1 + \frac{1}{4}u^2 \right). \quad (13)$$

Proposition 1 *The Fisher-Rao distance $\rho_{\mathcal{N}}((\mu_1, \Sigma), (\mu_2, \Sigma))$ between two MVNs with same covariance matrix is*

$$\begin{aligned} \rho_{\mathcal{N}}((\mu_1, \Sigma), (\mu_2, \Sigma)) &= \sqrt{2} \log \left(\frac{\sqrt{8 + \Delta_{\Sigma}^2(\mu_1, \mu_2)} + \Delta_{\Sigma}(\mu_1, \mu_2)}{\sqrt{8 + \Delta_{\Sigma}^2(\mu_1, \mu_2)} - \Delta_{\Sigma}(\mu_1, \mu_2)} \right) = \rho_{\mathcal{N}}((0, 1), (\Delta_{\Sigma}(\mu_1, \mu_2), 1)) \\ &= \sqrt{2} \operatorname{arccosh} \left(1 + \frac{1}{4}\Delta_{\Sigma}^2(\mu_1, \mu_2) \right), \end{aligned} \quad (15)$$

where $\Delta_{\Sigma}(\mu_1, \mu_2) = \sqrt{(\mu_2 - \mu_1)^{\top} \Sigma^{-1} (\mu_2 - \mu_1)}$ is the Mahalanobis distance.

Indeed, notice that the d -variate Mahalanobis distance $\Delta_{\Sigma}(\mu_1, \mu_2)$ can be interpreted as a univariate Mahalanobis distance between the standard normal distribution $N(0, 1)$ and $N(\Delta_{\Sigma}(\mu_1, \mu_2), 1)$:

$$\Delta_{\Sigma}(\mu_1, \mu_2) = \Delta_1(0, \Delta_{\Sigma}(\mu_1, \mu_2)).$$

Thus we have $\rho_{\mathcal{N}}((\mu_1, \Sigma), (\mu_2, \Sigma)) = \rho_{\mathcal{N}}((0, 1), (\Delta_{\Sigma}(\mu_1, \mu_2), 1))$, where the right hand-side term is the univariate Fisher-Rao distance of Eq. 4. Let us notice that the square length element on \mathcal{M}_{Σ} is $ds^2 = d\mu^{\top} \Sigma^{-1} d\mu = \Delta_{\Sigma}^2(\mu, \mu + d\mu)$.

Let us corroborate this result by checking formula of Eq. 1 with two examples in the literature: In [87] (Figure 4), we Fisher-Rao distance between $N_1 = (0, I)$ and $N_2 = \left(\begin{bmatrix} \frac{1}{2} \\ \frac{1}{2} \end{bmatrix}, I \right)$ is studied. We find $\rho_{\mathcal{N}}(N_1, N_2) = 0.69994085$ in accordance to their result shown in Figure 4. The second example is Example 1 of [76] (p. 11) with $N_1 = \left(\begin{bmatrix} -1 \\ 0 \end{bmatrix}, \Sigma \right)$ and $N_2 = \left(\begin{bmatrix} 6 \\ 3 \end{bmatrix}, \Sigma \right)$ for $\Sigma = \begin{bmatrix} 1.1 & 0.9 \\ 0.9 & 1.1 \end{bmatrix}$. Formula of Eq. 14 yields the Fisher-Rao distance 5.006483034546878 in accordance with [76] which reports 5.00648.

Similarly, the statistical Ali-Silvey-Csiszár f -divergences [3, 24]

$$I_f[p_{(\mu_1, \Sigma)} : p_{(\mu_2, \Sigma)}] = \int_{\mathbb{R}^d} p_{(\mu_1, \Sigma)}(x) f \left(\frac{p_{(\mu_2, \Sigma)}}{p_{(\mu_1, \Sigma)}} \right) dx,$$

between two MVNs sharing the same covariance matrix are increasing functions of the Mahalanobis distance because the f -divergences between two MVNs sharing the same covariance matrix are invariant under the action of the translation group [68]. Thus we have $I_f[p_{(\mu_1, \Sigma)} : p_{(\mu_2, \Sigma)}] = h_f(\Delta_{\Sigma}(\mu_1, \mu_2))$. Since $\Delta_{\Sigma}(\mu_1, \mu_2) = \Delta_1(0, \Delta_{\Sigma}(\mu_1, \mu_2))$, we thus have

$$I_f[p_{(\mu_1, \Sigma)} : p_{(\mu_2, \Sigma)}] = h_f(\Delta_1(0, \Delta_{\Sigma}(\mu_1, \mu_2))) = I_f[p_{(0,1)} : p_{(\Delta_{\Sigma}(\mu_1, \mu_2), 1)}],$$

where the right-hand side f -divergence is between univariate normal distributions. See Table 2 of [68] for some explicit functions h_f .

2 Calvo and Oller's family of diffeomorphic embeddings

Calvo and Oller [14, 15] noticed that we can embed the space of normal distributions in $\mathcal{P}(d+1)$ by using the following mapping:

$$f_\beta(N) = f_\beta(\mu, \Sigma) = \begin{bmatrix} \Sigma + \beta\mu\mu^\top & \beta\mu \\ \beta\mu^\top & \beta \end{bmatrix} \in \mathcal{P}(d+1), \quad (16)$$

where $\beta \in \mathbb{R}_{>0}$ and $N = N(\mu, \Sigma)$. Notice that since the dimension of $\mathcal{P}(d+1)$ is $\frac{(d+1)(d+2)}{2}$, we only use $\frac{(d+1)(d+2)}{2} - \frac{d(d+3)}{2} = 1$ extra dimension for embedding $\mathcal{N}(d)$ into $\mathcal{P}(d+1)$. By foliating $\mathbb{P} = \mathbb{R}_{>0} \times \mathbb{P}_c$ where $\mathbb{P}_c = \{P \in \mathbb{P} : |P| = c\}$ denotes the subsets of \mathbb{P} with determinant c , we get the following Riemannian Calvo & Oller metric on the SPD cone:

$$\begin{aligned} ds_{\text{CO}}^2 &= \frac{1}{2} \text{tr} \left((f^{-1}(\mu, \Sigma) df(\mu, \Sigma))^2 \right), \\ &= \frac{1}{2} \left(\frac{d\beta}{\beta} \right)^2 + \beta d\mu^\top \Sigma^{-1} d\mu + \frac{1}{2} \text{tr} \left((\Sigma^{-1} d\Sigma)^2 \right). \end{aligned}$$

Let

$$\bar{\mathcal{N}}_\beta(d) = \left\{ \bar{P} = f_\beta(\mu, \Sigma) : (\mu, \Sigma) \in \mathcal{N}(d) = \mathbb{R}^d \times \mathcal{P}(d) \right\}$$

denote the submanifold of $\mathcal{P}(d+1)$ of codimension 1, and $\bar{\mathcal{N}} = \bar{\mathcal{N}}_1$ (i.e., $\beta = 1$). The family of mappings f_β provides diffeomorphisms between $\mathcal{N}(d)$ and $\bar{\mathcal{N}}_\beta(d)$. Let $f_\beta^{-1}(\bar{P}) = (\mu_{\bar{P}}, \Sigma_{\bar{P}})$ denote the inverse mapping for $\bar{P} \in \bar{\mathcal{N}}_\beta(d)$, and let $f = f_1$ (i.e., $\beta = 1$): $f(\mu, \Sigma) = \begin{bmatrix} \Sigma + \mu\mu^\top & \mu \\ \mu^\top & 1 \end{bmatrix}$.

By equipping the cone $\mathcal{P}(d+1)$ by the trace metric [59, 65, 27] (also called the affine invariant Riemannian metric, AIRM) scaled by $\frac{1}{2}$:

$$g_P^{\text{trace}}(P_1, P_2) := \text{tr}(P^{-1}P_1P^{-1}P_2)$$

(yielding the squared line element $ds_{\mathcal{P}}^2 = \frac{1}{2} \text{tr}((P dP)^2)$), Calvo and Oller [14] proved that $\bar{\mathcal{N}}(d)$ is isometric to $\mathcal{N}(d)$ (i.e., the Riemannian metric of $\mathcal{P}(d+1)$ restricted to $\bar{\mathcal{N}}(d)$ coincides with the Riemannian metric of $\mathcal{N}(d)$ induced by f) but $\bar{\mathcal{N}}(d)$ is not totally geodesic (i.e., the geodesics $\gamma_{\mathcal{P}}(\bar{P}_1, \bar{P}_2; t)$ for $\bar{P}_1 = f(N_1), \bar{P}_2 = f(N_2) \in \bar{\mathcal{N}}(d)$ leaves the embedded normal submanifold $\bar{\mathcal{N}}(d)$). Note that g_P^{trace} can be interpreted as the Fisher metric for the family \mathcal{N}_0 of 0-centered normal distributions. Thus we have $(\mathcal{N}(d), g^{\text{Fisher}}) \hookrightarrow (\mathcal{P}(d+1), g^{\text{trace}})$, and the following diagram between parameter spaces and corresponding distributions:

$$\begin{array}{ccc} \mathcal{N}(d) & \hookrightarrow & \mathcal{N}_0(d+1) \\ \updownarrow & & \updownarrow \\ \Lambda(d) & \hookrightarrow & \mathbb{P}(d+1) \end{array}$$

Remark 5 *The trace metric was first studied by Siegel [82, 64] using the wider scope of complex symmetric matrices with positive-definite imaginary parts generalizing the Poincaré upper half-plane (see Appendix B).*

We omit to specify the dimensions and write for short \mathcal{N} , $\overline{\mathcal{N}}$ and \mathcal{P} when clear from context. Thus C&O proposed to use the embedding $f = f_1$ to give a lower bound ρ_{CO} of the Fisher-Rao distance $\rho_{\mathcal{N}}$ between normals:

$$\text{LC}_{\text{CO}} : \quad \rho_{\mathcal{N}}(N_1, N_2) \geq \rho_{\text{CO}}(\underbrace{f(\mu_1, \Sigma_1)}_{\bar{P}_1}, \underbrace{f(\mu_2, \Sigma_2)}_{\bar{P}_2}) = \sqrt{\frac{1}{2} \sum_{i=1}^{d+1} \log^2 \lambda_i(\bar{P}_1^{-1} \bar{P}_2)}. \quad (17)$$

We let $\rho_{\text{CO}}(N_1, N_2) = \rho_{\text{CO}}(f(N_1), f(N_2))$. The ρ_{CO} distance is invariant under affine transformations like the Fisher-Rao distance of Property 1:

Property 2 (affine-invariance of C&O distance [14]) *For all $A \in \text{GL}(d)$, $a \in \mathbb{R}^d$, we have $\rho_{\text{CO}}((A\mu_1 + a, A\Sigma_1 A^\top), (A\mu_2 + a, A\Sigma_2 A^\top)) = \rho_{\text{CO}}(N(\mu_1, \Sigma_1), N(\mu_2, \Sigma_2))$.*

When $\Sigma_1 = \Sigma_2 = \Sigma$, we have $|\bar{P}_1| = |\bar{P}_2| = |\Sigma|$. Since the Riemannian geodesics $\gamma_{\mathbb{P}}(P_1, P_2; t)$ in the SPD cone are given by $\gamma_{\mathbb{P}}(P_1, P_2; t) = P_1^{\frac{1}{2}}(P_1^{-\frac{1}{2}} P_2 P_1^{-\frac{1}{2}})^t P_1^{\frac{1}{2}}$ [5] (also written $\gamma_{\text{SPD}}(P_1, P_2; t)$), we have $|\gamma_{\mathbb{P}}(P_1, P_2; t)| = |\Sigma|$. Although the submanifold $\mathbb{P}_c = \{P \in \mathbb{P} : |P| = c\}$ is totally geodesic with respect to the trace metric, it is not totally geodesic with respect to $\frac{1}{2}\text{tr}((\bar{P}d\bar{P})^2)$. Thus although $\gamma_{\mathbb{P}}(P_1, P_2) \in \overline{\mathcal{N}}$, it does not correspond to the embedded MVN geodesics with respect to the Fisher metric. The C&O distance between two MVNs $N(\mu_1, \Sigma)$ and $N(\mu_2, \Sigma)$ sharing the same covariance matrix [14] is

$$\rho_{\text{CO}}(N(\mu_1, \Sigma), N(\mu_2, \Sigma)) = \text{arccosh} \left(1 + \frac{1}{2} \Delta_{\Sigma}^2(\mu_1, \mu_2) \right), \quad (18)$$

where $\text{arccosh}(x) := \log(x + \sqrt{x^2 - 1})$ for $x \geq 1$ and $\Delta_{\Sigma}(\mu_1, \mu_2)$ is the Mahalanobis distance between $N(\mu_1, \Sigma)$ and $N(\mu_2, \Sigma)$. In that case, we thus have $\rho_{\text{CO}}(N(\mu_1, \Sigma), N(\mu_2, \Sigma)) = h_{\text{CO}}(\Delta_{\Sigma}(\mu_1, \mu_2))$ where $h_{\text{CO}}(u) = \text{arccosh}(1 + \frac{1}{2}u^2)$ is a strictly monotone increasing function. Let us note in passing that in [14] (Corollary, page 230) there is a confusing or typographic error since the distance is reported as $\text{arccosh}(1 + \frac{1}{2}d_M(\mu_1, \mu_2))$ where d_M denotes ‘‘Mahalanobis distance’’ [54]. So either $d_M = \Delta_{\Sigma}^2$, Mahalanobis D^2 -distance, or there is a missing square in the equation of the Corollary page 230. To get a flavor of how good is the approximation of the C&O distance, we may consider the same-covariance case where we have both closed-form solutions for $\rho_{\mathcal{N}}$ (Eq. 15) and ρ_{CO} (Eq. 18). Figure 3 plots the two functions h_{CO} and h_{FR} (with $h_{\text{CO}}(u) \leq h_{\text{FR}}(u) \leq u$ for $u \in [0, \infty)$).

Let us remark that similarly all f -divergences between $N_1 = (\mu_1, \Sigma)$ and $N_2 = (\mu_2, \Sigma)$ are scalar functions of their Mahalanobis distance $\Delta_{\Sigma}(\mu_1, \mu_2)$ too, see [68].

The C&O distance ρ_{CO} is a metric distance that has been used in many applications ranging from computer vision [18, 92, 61, 58] to signal/sensor processing, statistics [47, 56], machine learning [88, 93, 50, 51, 74, 22] and analogical reasoning [60].

Remark 6 *In a second paper, Calvo and Oller [15] noticed that we can embed normal distributions in $\mathcal{P}(d+1)$ by the following more general mapping (Lemma 3.1 [15]):*

$$g_{\alpha, \beta, \gamma}(\mu, \Sigma) = |\Sigma|^{\alpha} \begin{bmatrix} \Sigma + \beta\gamma^2 \mu\mu^\top & \beta\gamma\mu \\ \beta\gamma\mu^\top & \beta \end{bmatrix} \in \mathcal{P}(d+1), \quad (19)$$

Distances as functions of the Mahalanobis distance

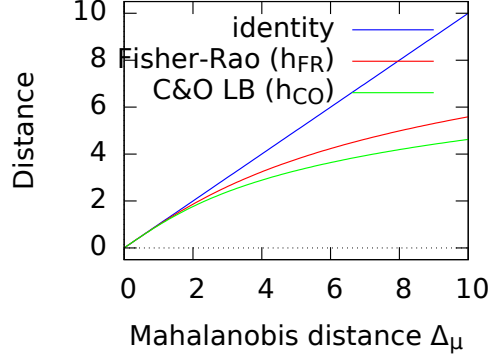


Figure 3: Quality of the C&O lower bound compared to the exact Fisher-Rao distance in the case of $N_1, N_2 \in \mathcal{M}_\Sigma$ (MVNs sharing the same covariance matrix Σ). We have $\rho_{\text{CO}} \leq \rho_{\mathcal{N}} \leq \Delta_\Sigma$.

where $\alpha \in \mathbb{R}$, $\beta \in \mathbb{R}_{>0}$ and $\gamma \in \mathbb{R}$. It is show in [15] that the induced length element is

$$ds_{\alpha,\beta,\gamma}^2 = \frac{1}{2} \left(\alpha((d+1) + 2\alpha)\text{tr}^2(\Sigma^{-1}d\Sigma) + \text{tr}((\Sigma^{-1}d\Sigma)^2) + 2\beta\gamma^2 d\mu^\top \Sigma^{-1}d\mu + 2\alpha \text{tr}(\Sigma^{-1}d\Sigma) \frac{d\beta}{\beta} + \left(\frac{d\beta}{\beta}\right)^2 \right).$$

When $\gamma = \beta = 1$, we have

$$ds_\alpha^2 = \frac{1}{2} \left(\alpha((d+1) + 2\alpha)\text{tr}^2(\Sigma^{-1}d\Sigma) + \text{tr}((\Sigma^{-1}d\Sigma)^2) + 2\beta\gamma^2 d\mu^\top \Sigma^{-1}d\mu \right).$$

Thus to cancel the term $\text{tr}^2(\Sigma^{-1}d\Sigma)$, we may either choose $\alpha = 0$ or $\alpha = -\frac{2}{1+d}$.

In some applications [77], the embedding

$$g_{-\frac{1}{d+1},1,1}(\mu, \Sigma) = |\Sigma|^{-\frac{1}{d+1}} \begin{bmatrix} \Sigma + \mu\mu^\top & \mu \\ \mu^\top & 1 \end{bmatrix} := \hat{f}(\mu, \Sigma), \quad (20)$$

is used to ensure that $|g_{-\frac{1}{d+1},1,1}(\mu, \Sigma)| = 1$. That is normal distributions are embedded diffeomorphically into the submanifold of positive-definite matrices with unit determinant (also called SSPD, acronym of Special SPD). In [15], C&O showed that there exists a second isometric embedding of the Fisher-Rao Gaussian manifold $\mathcal{N}(d)$ into a submanifold of the cone $\mathcal{P}(d+1)$:

$f_{\text{SSPD}}(\mu, \Sigma) = |\Sigma|^{-\frac{2}{d+1}} \begin{bmatrix} \Sigma + \mu\mu^\top & \mu \\ \mu^\top & 1 \end{bmatrix}$. Let $\hat{P} = f_{\text{SSPD}}(\mu, \Sigma)$. This mapping can be understood as taking the elliptic isometry $P \mapsto |P|^{-\frac{2}{d+1}} P$ of $P \in \mathcal{P}(d+1)$ [27] since $|\Sigma| = |\bar{P}(\mu, \Sigma)|$ (see proof in Proposition 3). It follows that

$$\rho_{\text{CO}}(N_1, N_2) = \rho_{\mathcal{P}}(\bar{P}_1, \bar{P}_2) = \rho_{\mathcal{P}}(\hat{P}_1, \hat{P}_2) \leq \rho_{\mathcal{N}}(N_1, N_2).$$

Similarly, we could have mapped $P \mapsto P^{-1}$ to get another isometric embedding. See the four types of elliptic isometric of the SPD cone described in [27]. Finally, let us remark that the SSPD submanifold is totally geodesic with respect to the trace metric but not with respect to the C&O metric.

The multivariate Gaussian manifold $\mathcal{N}(d)$ can also be embedded into the SPD cone $\mathcal{P}(d+1)$ as a Riemannian symmetric space [53, 35] by f_{SSPD} : $\hat{\mathcal{P}} = \{f_{\text{SSPD}}(N) \in \mathcal{P}(d+1) : N \in \mathcal{N}(d)\}$. We have $\hat{\mathcal{P}} \cong \text{SL}(d+1)/\text{SO}(d+1)$ [53, 30, 31] (and textbook [10], Part II Chapter 10), and the symmetric space $\text{SL}(d+1)/\text{SO}(d+1)$ can be embedded with the Killing Riemannian metric instead of the Fisher information metric:

$$g^{\text{Killing}}(N_1, N_2) = \kappa_{\text{Killing}} \left(\mu_1^\top \Sigma^{-1} \mu_2 + \frac{1}{2} \text{tr} (\Sigma^{-1} \Sigma_1 \Sigma^{-1} \Sigma_2) - \frac{1}{2(d+1)} \text{tr} (\Sigma^{-1} \Sigma_1) \text{tr} (\Sigma^{-1} \Sigma_2) \right),$$

where $\kappa_{\text{Killing}} > 0$ is a predetermined constant (e.g. 1). The length element of the Killing metric is

$$ds_{\text{SS}}^2 = \kappa_{\text{Killing}} \left(\frac{1}{2} d\mu^\top \Sigma^{-1} d\mu + \text{tr} \left((\Sigma^{-1} d\Sigma)^2 \right) - \frac{1}{2} \text{tr}^2 (\Sigma^{-1} d\Sigma) \right).$$

When we consider \mathcal{N}_Σ , we may choose $\kappa_{\text{Killing}} = 2$ so that the Killing metric coincides with the Fisher information metric. The induced Killing distance [53] is available in closed form:

$$\rho_{\text{Killing}}(N_1, N_2) = \sqrt{\kappa_{\text{Killing}} \sum_{i=1}^{d+1} \log^2 \lambda_i \left(\hat{L}_1^{-1} \hat{P}_2 \left(\hat{L}_1^{-1} \right)^\top \right)}, \quad (21)$$

where \hat{L}_1 is the unique lower triangular matrix obtained from the Cholesky decomposition of $\hat{P}_1 = f_{\text{SSPD}}(N_1) = \hat{L}_1 \hat{L}_1^\top$. Note that $\hat{L}_1^{-1} \hat{P}_2 \left(\hat{L}_1^{-1} \right)^\top \in \mathcal{P}(d+1)$ and $|\hat{L}_1|$, i.e., $\hat{L}_1 \in \text{SL}(d+1)$.

When $N_1 = (\mu_1, \Sigma)$ and $N_2 = (\mu_2, \Sigma)$ ($N_1, N_2 \in \mathcal{N}_\Sigma$), we have [53]

$$\rho_{\text{Killing}}(N_1, N_2) = \sqrt{2\kappa_{\text{Killing}} \text{arccosh} \left(1 + \frac{1}{2} \Delta_\Sigma^2(\mu_1, \mu_2) \right)},$$

where Δ_Σ^2 is the squared Mahalanobis distance. Thus $\rho_{\text{Killing}}(N_1, N_2) = h_{\text{Killing}}(\Delta_\Sigma(\mu_1, \mu_2))$ where $h_{\text{Killing}}(u) = \sqrt{2\kappa_{\text{Killing}} \text{arccosh} \left(1 + \frac{1}{2} u^2 \right)}$.

When $N_1 = (\mu, \Sigma_1)$ and $N_2 = (\mu, \Sigma_2)$ ($N_1, N_2 \in \mathcal{N}_\mu$), we have [53]:

$$\rho_{\text{Killing}}(N_1, N_2) = \sqrt{\kappa_{\text{Killing}} \left(\sum_{i=1}^d \log^2 \lambda_i \left(L_1^{-1} P_2 \left(L_1^{-1} \right)^\top \right) - \frac{1}{(d+1)^2} \left(\sum_{i=1}^d \log \lambda_i \left(L_1^{-1} P_2 \left(L_1^{-1} \right)^\top \right) \right)^2 \right)}.$$

See Example 1. Let us emphasize that the Killing distance is not the Fisher-Rao distance but is available in closed-form as an alternative metric distance between MVNs.

3 Approximating the Fisher-Rao distance

3.1 Approximating length of curves

Rao's distance [57] is a Riemannian geodesic distance

$$\rho_{\mathcal{N}}(p_{\lambda_1}, p_{\lambda_2}) = \inf_c \{ \text{Length}(c) : c(0) = p_{\lambda_1}, c(1) = p_{\lambda_2} \},$$

where

$$\text{Length}(c) = \int_0^1 \underbrace{\sqrt{\langle \dot{c}(t), \dot{c}(t) \rangle_{c(t)}}}_{ds_{\mathcal{N}}(t)} dt.$$

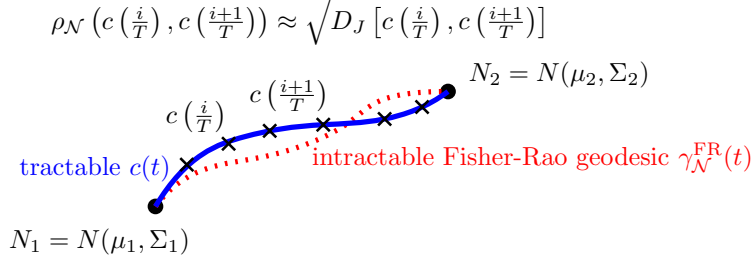


Figure 4: Approximating the Fisher-Rao geodesic distance $\rho_{\mathcal{N}}(N_1, N_2)$: The Fisher-Rao geodesic $\gamma_{\mathcal{N}}^{\text{FR}}$ is not known in closed-form. We consider a tractable curve $c(t)$, discretize $c(t)$ at $T + 1$ points $c(\frac{i}{T})$ with $c(0) = N_1$ and $c(1) = N_2$, and approximate $\rho_{\mathcal{N}}(c(\frac{i}{T}), c(\frac{i+1}{T}))$ by $D_J[c(\frac{i}{T}), c(\frac{i+1}{T})]$. Considering different tractable curves $c(t)$ yield different approximations.

We can approximate the Rao distance $\rho_{\mathcal{N}}(N_1, N_2)$ by discretizing regularly any smooth curve $c(t)$ joining N_1 ($t = 0$) to N_2 ($t = 1$):

$$\rho_{\mathcal{N}}(N_1, N_2) \leq \frac{1}{T} \sum_{i=1}^{T-1} \rho_{\mathcal{N}}\left(c\left(\frac{i}{T}\right), c\left(\frac{i+1}{T}\right)\right),$$

with equality holding iff $c(t) = \gamma_{\mathcal{N}}(N_1, N_2; t)$ is the Riemannian geodesic induced by the Fisher information metric.

When T is sufficiently large, the normal distributions $c(\frac{i}{T})$ and $c(\frac{i+1}{T})$ are close to each other, and we can approximate $\rho_{\mathcal{N}}(c(\frac{i}{T}), c(\frac{i+1}{T}))$ by $\sqrt{D_J[c(\frac{i}{T}), c(\frac{i+1}{T})]}$, where $D_J[N_1, N_2] = D_{\text{KL}}[N_1, N_2] + D_{\text{KL}}[N_2, N_1]$ is Jeffreys divergence, and D_{KL} is the Kullback-Leibler divergence:

$$D_{\text{KL}}[p_{(\mu_1, \Sigma_1)} : p_{(\mu_2, \Sigma_2)}] = \frac{1}{2} \left(\text{tr}(\Sigma_2^{-1} \Sigma_1) + \Delta \mu^\top \Sigma_2^{-1} \Delta \mu - d + \log \frac{|\Sigma_2|}{|\Sigma_1|} \right).$$

Thus the costly determinant computations cancel each others in Jeffreys divergence (i.e., $\log \frac{|\Sigma_2|}{|\Sigma_1|} + \log \frac{|\Sigma_1|}{|\Sigma_2|} = 0$) and we have:

$$D_J[p_{(\mu_1, \Sigma_1)} : p_{(\mu_2, \Sigma_2)}] = \text{tr} \left(\frac{\Sigma_2^{-1} \Sigma_1 + \Sigma_1^{-1} \Sigma_2}{2} - I \right) + \Delta \mu^\top \frac{\Sigma_1^{-1} + \Sigma_2^{-1}}{2} \Delta \mu.$$

Figure 4 summarizes our method to approximate the Fisher-Rao geodesic distance.

In general, it holds that $I_f[p : q] \approx \frac{f''(1)}{2} ds_{\text{Fisher}}^2$ between infinitesimally close distributions p and q ($ds \approx \sqrt{\frac{2I_f[p:q]}{f''(1)}}$), where $I_f[\cdot : \cdot]$ denotes a f -divergence [4]. The Jeffreys divergence is a f -divergence obtained for $f_J(u) = -\log u + u \log u$ with $f_J''(1) = 2$. It is thus interesting to find low computational cost f -divergences between multivariate normal distributions in order to approximate the infinitesimal length element ds . Note that f -divergences between MVNs are invariant under the action of the affine group [68]. Thus for infinitesimally close distributions p and q , this informally explains that ds_{Fisher} is invariant under the action of the affine group.

Although the definite integral of the length element along the Fisher-Rao geodesic $\gamma_{\mathcal{N}}^{\text{FR}}$ is not known in closed form (i.e., Fisher-Rao distance), the integral of the squared length element along the mixture geodesic $\gamma_{\mathcal{N}}^m$ and exponential geodesic $\gamma_{\mathcal{N}}^e$ coincide with Jeffreys divergence [4]:

Property 3 ([4]) *We have*

$$D_J[p_{\lambda_1}, p_{\lambda_2}] = \int_0^1 ds_{\mathcal{N}}^2(\gamma_{\mathcal{N}}^m(p_{\lambda_1}, p_{\lambda_2}; t))dt = \int_0^1 ds_{\mathcal{N}}^2(\gamma_{\mathcal{N}}^e(p_{\lambda_1}, p_{\lambda_2}; t))dt.$$

Proof: Let us report a proof of this remarkable fact in the general setting of Bregman manifolds (proof omitted in [4]). Since $D_J[p_{\lambda_1}, p_{\lambda_2}] = D_{\text{KL}}[p_{\lambda_1}, p_{\lambda_2}] + D_{\text{KL}}[p_{\lambda_2}, p_{\lambda_1}]$ and $D_{\text{KL}}[p_{\lambda_1}, p_{\lambda_2}] = B_F(\theta(\lambda_2) : \theta(\lambda_1))$, where B_F denotes the Bregman divergence induced by the cumulant function of the multivariate normals and $\theta(\lambda)$ is the natural parameter corresponding to λ , we have

$$\begin{aligned} D_J[p_{\lambda_1}, p_{\lambda_2}] &= B_F(\theta_1 : \theta_2) + B_F(\theta_2 : \theta_1), \\ &= S_F(\theta_1; \theta_2) = (\theta_2 - \theta_1)^\top (\eta_2 - \eta_1) = S_{F^*}(\eta_1; \eta_2), \end{aligned}$$

where $\eta = \nabla F(\theta)$ and $\theta = \nabla F^*(\eta)$ denote the dual parameterizations obtained by the Legendre-Fenchel convex conjugate $F^*(\eta)$ of $F(\theta)$. The proof is based on the first-order and second-order directional derivatives. The first-order directional derivative $\nabla_u F(\theta)$ with respect to vector u is defined by

$$\nabla_u F(\theta) = \lim_{t \rightarrow 0} \frac{F(\theta + tv) - F(\theta)}{t} = v^\top \nabla F(\theta).$$

The second-order directional derivatives $\nabla_{u,v}^2 F(\theta)$ is

$$\begin{aligned} \nabla_{u,v}^2 F(\theta) &= \nabla_u \nabla_v F(\theta), \\ &= \lim_{t \rightarrow 0} \frac{v^\top \nabla F(\theta + tu) - v^\top \nabla F(\theta)}{t}, \\ &= u^\top \nabla^2 F(\theta) v. \end{aligned}$$

Now consider the squared length element $ds^2(\gamma(t))$ on the primal geodesic $\gamma(t)$ expressed using the primal coordinate system θ : $ds^2(\gamma(t)) = d\theta(t)^\top \nabla^2 F(\theta(t)) d\theta(t)$ with $\theta(\gamma(t)) = \theta_1 + t(\theta_2 - \theta_1)$ and $d\theta(t) = \theta_2 - \theta_1$. Let us express the $ds^2(\gamma(t))$ using the second-order directional derivative:

$$ds^2(\gamma(t)) = \nabla_{\theta_2 - \theta_1}^2 F(\theta(t)).$$

Thus we have $\int_0^1 ds^2(\gamma(t))dt = [\nabla_{\theta_2 - \theta_1} F(\theta(t))]_0^1$, where the first-order directional derivative is $\nabla_{\theta_2 - \theta_1} F(\theta(t)) = (\theta_2 - \theta_1)^\top \nabla F(\theta(t))$. Therefore we get $\int_0^1 ds^2(\gamma(t))dt = (\theta_2 - \theta_1)^\top (\nabla F(\theta_2) - \nabla F(\theta_1)) = S_F(\theta_1; \theta_2)$.

Similarly, we express the squared length element $ds^2(\gamma^*(t))$ using the dual coordinate system η as the second-order directional derivative of $F^*(\eta(t))$ with $\eta(\gamma^*(t)) = \eta_1 + t(\eta_2 - \eta_1)$:

$$ds^2(\gamma^*(t)) = \nabla_{\eta_2 - \eta_1}^2 F^*(\eta(t)).$$

Therefore, we have $\int_0^1 ds^2(\gamma^*(t))dt = [\nabla_{\eta_2 - \eta_1} F^*(\eta(t))]_0^1 = S_{F^*}(\eta_1; \eta_2)$. Since $S_{F^*}(\eta_1; \eta_2) = S_F(\theta_1; \theta_2)$, we conclude that

$$S_F(\theta_1; \theta_2) = \int_0^1 ds^2(\gamma(t))dt = \int_0^1 ds^2(\gamma^*(t))dt$$

In 1D, both pregeodesics $\gamma(t)$ and $\gamma^*(t)$ coincide. We have $ds^2(t) = (\theta_2 - \theta_1)^2 f''(\theta(t)) = (\eta_2 - \eta_1) f^{*''}(\eta(t))$ so that we check that $S_F(\theta_1; \theta_2) = \int_0^1 ds^2(\gamma(t))dt = (\theta_2 - \theta_1) [f'(\theta(t))]_0^1 = (\eta_2 - \eta_1) [f^{*'}(\eta(t))]_0^1 = (\eta_2 - \eta_1)(\theta_2 - \theta_1)$. \square

It follows the following property:

Property 4 (Fisher-Rao upper bound) *The Fisher-Rao distance between normal distributions is upper bounded by the square root of the Jeffreys divergence: $\rho_{\mathcal{N}}(N_1, N_2) \leq \sqrt{D_J(N_1, N_2)}$.*

Proof: Consider the Cauchy-Schwarz inequality for positive functions $f(t)$ and $g(t)$: $\int_0^1 f(t)g(t)dt \leq \sqrt{(\int_0^1 f(t)^2 dt)(\int_0^1 g(t)^2 dt)}$, and let $f(t) = ds_{\mathcal{N}}(\gamma_{\mathcal{N}}^c(p_{\lambda_1}, p_{\lambda_2}; t))$ and $g(t) = 1$. Then we get:

$$\left(\int_0^1 ds_{\mathcal{N}}(\gamma_{\mathcal{N}}^c(p_{\lambda_1}, p_{\lambda_2}; t)) dt \right)^2 \leq \left(\int_0^1 ds_{\mathcal{N}}^2(\gamma_{\mathcal{N}}^c(p_{\lambda_1}, p_{\lambda_2}; t)) dt \right) \left(\int_0^1 1^2 dt \right)$$

Furthermore since by definition of $\gamma_{\mathcal{N}}^{\text{FR}}$, we have

$$\int_0^1 ds_{\mathcal{N}}(\gamma_{\mathcal{N}}^c(p_{\lambda_1}, p_{\lambda_2}; t)) dt \geq \int_0^1 ds_{\mathcal{N}}(\gamma_{\mathcal{N}}^{\text{FR}}(p_{\lambda_1}, p_{\lambda_2}; t)) dt =: \rho_{\mathcal{N}}(N_1, N_2),$$

it follows for $c = e$ (i.e., e -geodesic $\gamma_{\mathcal{N}}^e$), we have:

$$\rho_{\mathcal{N}}(N_1, N_2)^2 \leq \int_0^1 ds_{\mathcal{N}}^2(\gamma_{\mathcal{N}}^e(p_{\lambda_1}, p_{\lambda_2}; t)) dt = D_J(N_1, N_2).$$

Thus we have $\rho_{\mathcal{N}}(N_1, N_2) \leq \sqrt{D_J(N_1, N_2)}$.

Note that in Riemannian geometry, a curve γ minimizes the energy $E(\gamma) = \int_0^1 |\dot{\gamma}(t)|^2 dt$ if it minimizes the length $L(\gamma) = \int_0^1 \|\dot{\gamma}(t)\| dt$ and $\|\dot{\gamma}(t)\|$ is constant. Using Cauchy-Schwartz inequality, we can show that $L(\gamma) \leq E(\gamma)$. \square

Note that this upper bound is tight at infinitesimal scale (i.e., when $N_2 = N_1 + dN$).

For any smooth curve $c(t)$, we thus approximate $\rho_{\mathcal{N}}$ by

$$\boxed{\tilde{\rho}_{\mathcal{N}}^c(N_1, N_2) := \frac{1}{T} \sum_{i=1}^{T-1} \sqrt{D_J \left[c \left(\frac{i}{T} \right), c \left(\frac{i+1}{T} \right) \right]}.} \quad (22)$$

For example, we may consider the following curves on \mathcal{N} which admit closed-form parameterizations in $t \in [0, 1]$:

- linear interpolation $c_{\lambda}(t) = t(\mu_1, \Sigma_1) + (1-t)(\mu_2, \Sigma_2)$ between (μ_1, Σ_1) and (μ_2, Σ_2) ,
- the mixture geodesic [63] $c_m(t) = \gamma_{\mathcal{N}}^m(N_1, N_2; t) = (\mu_t^m, \Sigma_t^m)$ with $\mu_t^m = \bar{\mu}_t$ and $\Sigma_t^m = \bar{\Sigma}_t + t\mu_1\mu_1^{\top} + (1-t)\mu_2\mu_2^{\top} - \bar{\mu}_t\bar{\mu}_t^{\top}$ where $\bar{\mu}_t = t\mu_1 + (1-t)\mu_2$ and $\bar{\Sigma}_t = t\Sigma_1 + (1-t)\Sigma_2$,
- the exponential geodesic [63] $c_e(t) = \gamma_{\mathcal{N}}^e(N_1, N_2; t) = (\mu_t^e, \Sigma_t^e)$ with $\mu_t^e = \bar{\Sigma}_t^H (t\Sigma_1^{-1}\mu_1 + (1-t)\Sigma_2^{-1}\mu_2)$ and $\Sigma_t^e = \bar{\Sigma}_t^H$ where $\bar{\Sigma}_t^H = (t\Sigma_1^{-1} + (1-t)\Sigma_2^{-1})^{-1}$ is the matrix harmonic mean,
- the curve $c_{em}(t) = \frac{1}{2}(\gamma_{\mathcal{N}}^e(N_1, N_2; t) + \gamma_{\mathcal{N}}^m(N_1, N_2; t))$ which is obtained by averaging the mixture geodesic with the exponential geodesic.

Let us denote by $\tilde{\rho}_{\mathcal{N}}^{\lambda} = \tilde{\rho}_{\mathcal{N}}^{c_{\lambda}}$, $\tilde{\rho}_{\mathcal{N}}^m = \tilde{\rho}_{\mathcal{N}}^{c_m}$, $\tilde{\rho}_{\mathcal{N}}^e = \tilde{\rho}_{\mathcal{N}}^{c_e}$ and $\tilde{\rho}_{\mathcal{N}}^{em} = \tilde{\rho}_{\mathcal{N}}^{c_{em}}$ the approximations obtained by these curves following from Eq. 22. Figure 5 visualizes the exponential and mixture geodesics between two bivariate normal distributions. When T is sufficiently large, the approximated distances $\tilde{\rho}^x$ are close to the length of curve x , and we may thus consider several curves c_i and report the smallest Fisher-Rao distance approximations obtained: $\rho_{\mathcal{N}}(N_1, N_2) \approx \min_i \tilde{\rho}_{\mathcal{N}}^{c_i}(N_1, N_2)$.

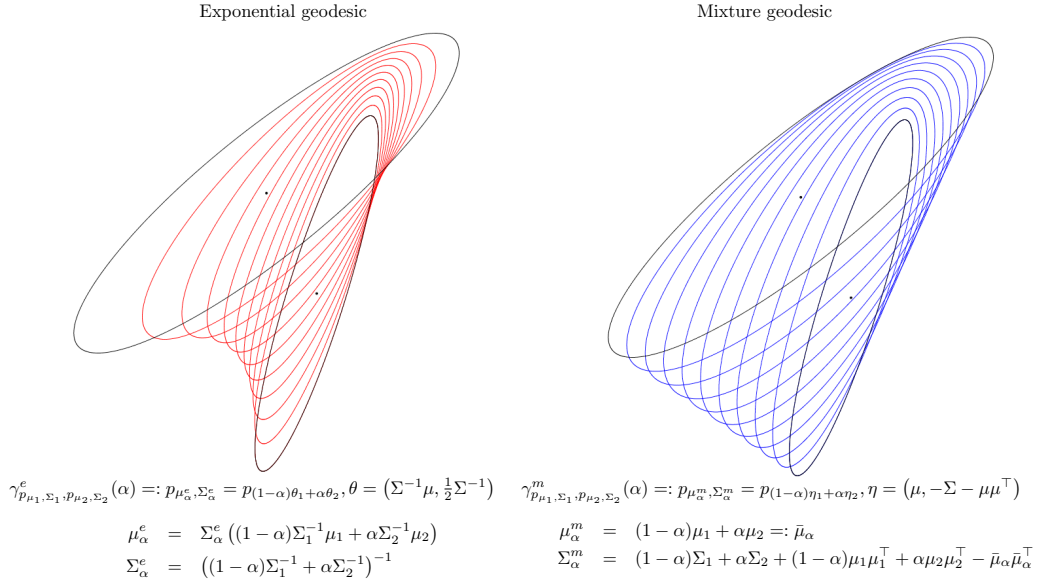


Figure 5: Visualizing the exponential and mixture geodesics between two bivariate normal distributions.

Note that we consider the regular spacing for approximating a curve length and do not optimize the position of the sample points on the curve. Indeed, as $T \rightarrow \infty$, the curve length approximation tends to the Riemannian curve length. In other words, we can measure approximately finely the length of any curve available with closed-form reparameterization by increasing T . Thus the key question of our method is how to best approximate the Fisher-Rao geodesic by a closed-form curve.

Remark 7 In [35], the authors consider the embedding of Eq. 20 and use the Killing metric g^{Killing} instead of the Fisher metric defined by:

$$g_N^{\text{Killing}}(N_1, N_2) = \mu_1^\top \Sigma^{-1} \mu_2 + \frac{1}{2} \text{tr}(\Sigma^{-1} \Sigma_1 \Sigma^{-1} \Sigma_2) - \frac{1}{2(d+1)} \text{tr}(\Sigma^{-1} \Sigma_1) \text{tr}(\Sigma^{-1} \Sigma_2),$$

where $N = (\mu, \Sigma)$, $N_1 = (\mu_1, \Sigma_1)$, and $N_2 = (\mu_2, \Sigma_2)$. A Fisher geodesic defect measure of a curve c is defined by

$$\delta(c) = \lim_{s \rightarrow \infty} \frac{1}{s} \int_0^s \|\nabla_{\dot{c}}^{g^{\text{Fisher}}} \dot{c}\|_{c(t)}^{\text{Fisher}} dt,$$

where $\nabla^{g^{\text{Fisher}}}$ denotes the Levi-Civita connection induced by the Fisher metric. When $\delta(c) = 0$ the curve is said an asymptotic geodesic of the Fisher geodesic. It is proven that Killing geodesics at (μ, Σ) are asymptotic Fisher geodesics when the initial condition $c'(0)$ is orthogonal to \mathcal{N}_μ .

Next, we introduce yet another curve $c_{\text{CO}}(t)$ derived from Calvo & Oller isometric mapping f which experimentally behaves better when normals are not *too far* from each others.

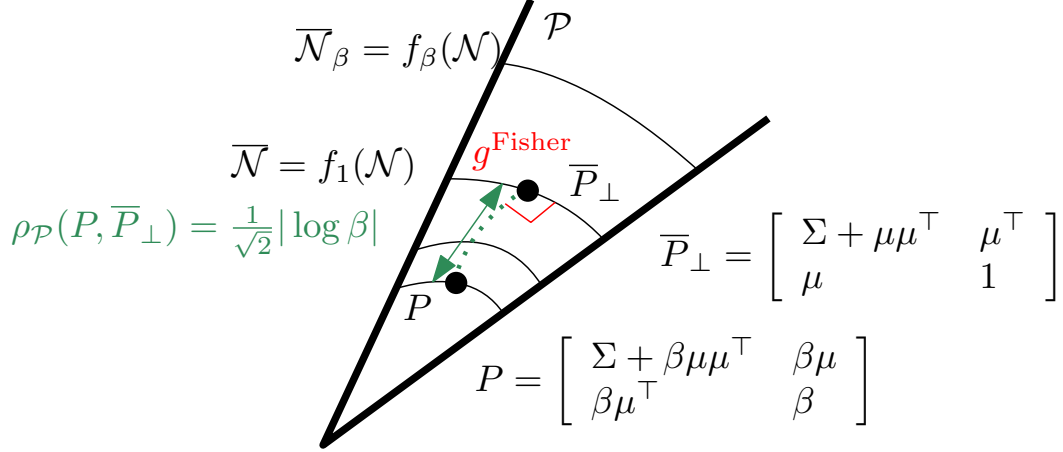


Figure 6: Projecting a SPD matrix $P \in \mathcal{P}$ onto $\bar{\mathcal{N}} = f(\mathcal{N})$.

3.2 Calvo & Oller's curve

This approximation consists in leveraging the closed-form expression of the SPD geodesics [59, 5]:

$$\gamma_{\mathcal{P}}(P, Q; t) = P^{\frac{1}{2}} \left(P^{-\frac{1}{2}} Q^{\frac{1}{2}} P^{-\frac{1}{2}} \right)^t P^{\frac{1}{2}},$$

to approximate the Fisher-Rao normal geodesic $\gamma_{\mathcal{N}}(N_1, N_2; t)$ as follows: Let $\bar{P}_1 = f(N_1), \bar{P}_2 = f(N_2) \in \bar{\mathcal{N}}$, and consider the smooth curve

$$\bar{c}_{\text{CO}}(P_1, P_2; t) = \text{proj}_{\bar{\mathcal{N}}}(\gamma_{\mathcal{P}}(\bar{P}_1, \bar{P}_2; t)),$$

where $\text{proj}_{\bar{\mathcal{N}}}(P)$ denotes the Fisher orthogonal projection of $P \in \mathcal{P}(d+1)$ onto $\bar{\mathcal{N}}$ (Figure 8). Thus curve c_{CO} is then defined as $f^{-1}(\bar{c}_{\text{CO}})$. Note that the power matrix P^t is $U \text{diag}(\lambda_1^t, \dots, \lambda_d^t) V^T$ where $P = U \text{diag}(\lambda_1^t, \dots, \lambda_d^t) V^T$ is the eigenvalue decomposition of P .

Let us now explain how to project $P = [P_{i,j}] \in \mathcal{P}(d+1)$ onto $\bar{\mathcal{N}}$ based on the analysis of the Appendix of [14] (page 239):

Proposition 2 (Projection of a SPD matrix onto the embedded normal submanifold $\bar{\mathcal{N}}$)

Let $\beta = P_{d+1,d+1}$ and write $P = \begin{bmatrix} \Sigma + \beta \mu \mu^T & \beta \mu \\ \beta \mu^T & \beta \end{bmatrix}$. Then the orthogonal projection at $P \in \mathcal{P}$ onto $\bar{\mathcal{N}}$ is:

$$\bar{P}_{\perp} = \text{proj}_{\bar{\mathcal{N}}}(P) = \begin{bmatrix} \Sigma + \mu \mu^T & \mu^T \\ \mu & 1 \end{bmatrix},$$

and the SPD distance between P and \bar{P}_{\perp} is $\rho_{\mathcal{P}}(P, \bar{P}_{\perp}) = \frac{1}{\sqrt{2}} |\log \beta|$.

Remark 8 In Diffusion Tensor Imaging [40] (DTI), the Fisher-Rao distance can be used to evaluate the distance between 3D normal distributions with means located at a 3D grid position. We may consider $3 \times 3 \times 3 - 1 = 26$ neighbor graphs induced by the grid, and for each normal N of the grid, calculate the approximations of the Fisher-Rao distance of N with its neighbors N' as depicted in Figure 7. Then the distance between two tensors N_1 and N_2 of the 3D grid is calculated as the shortest path on the weighted graph using Dijkstra's algorithm [40].

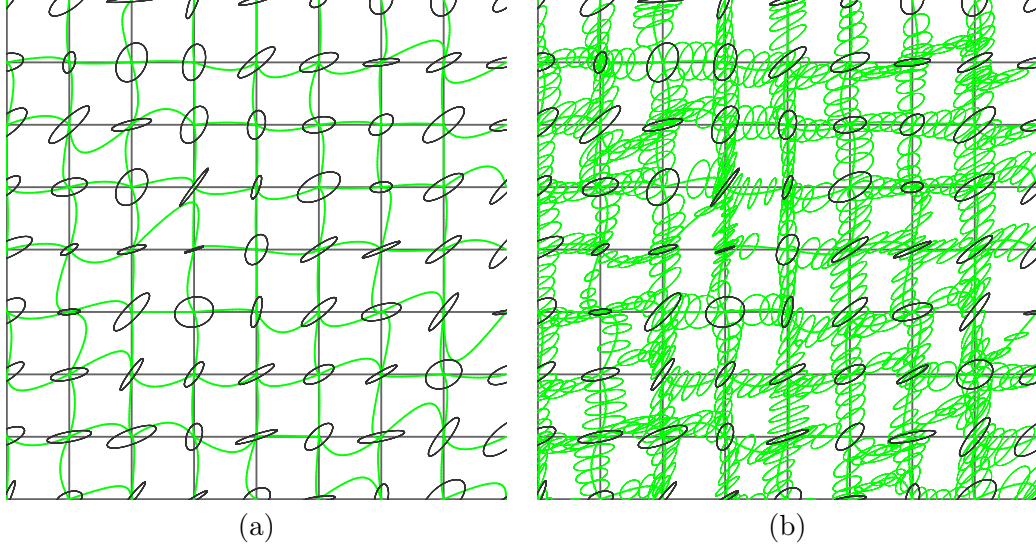


Figure 7: Diffusion tensor imaging on a 2D grid: (a) Ellipsoids shown at the 8×8 grid locations with C&O curves in green, and (b) some interpolated ellipsoids are further shown along the C&O curves.

Note that the Fisher-Rao projection of $N = (\mu, \Sigma)$ on a submanifold with fixed mean μ_0 was recently reported in closed-form in [88].

Let $\bar{c}_{\text{CO}}(t) = \bar{S}_t$ and $c_{\text{CO}}(t) = f^{-1}(c_{\text{CO}}(t)) =: G_t$. The following proposition shows that we have $D_J[\bar{S}_t, \bar{S}_{t+1}] = D_J[G_t, G_{t+1}]$.

Proposition 3 *The Kullback-Leibler divergence between p_{μ_1, Σ_1} and p_{μ_2, Σ_2} amounts to the KLD between $q_{\bar{P}_1} = p_{0, f(\mu_1, \Sigma_1)}$ and $q_{\bar{P}_2} = p_{0, f(\mu_2, \Sigma_2)}$ where $\bar{P}_i = f(\mu_i, \Sigma_i)$:*

$$D_{\text{KL}}[p_{\mu_1, \Sigma_1} : p_{\mu_2, \Sigma_2}] = D_{\text{KL}}[q_{\bar{P}_1} : q_{\bar{P}_2}].$$

Proof: The KLD between two centered $(d+1)$ -variate normals $q_{P_1} = p_{0, P_1}$ and $q_{P_2} = p_{0, P_2}$ is

$$D_{\text{KL}}[q_{P_1} : q_{P_2}] = \frac{1}{2} \left(\text{tr}(P_2^{-1} P_1) - d - 1 + \log \frac{|P_2|}{|P_1|} \right).$$

This divergence can be interpreted as the matrix version of the Itakura-Saito divergence [25]. The SPD cone equipped with $\frac{1}{2}$ of the trace metric can be interpreted as Fisher-Rao centered normal manifolds: $(\mathcal{N}_\mu, g_{\mathcal{N}_\mu}^{\text{Fisher}}) = (\mathcal{P}, \frac{1}{2} g^{\text{trace}})$.

Since the determinant of a block matrix is

$$\left| \begin{bmatrix} A & B \\ C & D \end{bmatrix} \right| = |A - BD^{-1}C|,$$

we get with $D = 1$: $|f(\mu, \Sigma)| = |\Sigma + \mu\mu^\top - \mu\mu^\top| = |\Sigma|$.

Let $\bar{P}_1 = f(\mu_1, \Sigma_1)$ and $\bar{P}_2 = f(\mu_2, \Sigma_2)$. Checking $D_{\text{KL}}[p_{\mu_1, \Sigma_1} : p_{\mu_2, \Sigma_2}] = D_{\text{KL}}[q_{\bar{P}_1} : q_{\bar{P}_2}]$ where $q_{\bar{P}} = p_{0, \bar{P}}$ amounts to verify that

$$\text{tr}(\bar{P}_2^{-1} \bar{P}_1) = 1 + \text{tr}(\Sigma_2^{-1} \Sigma_1 + \Delta_\mu^\top \Sigma_2^{-1} \Delta_\mu).$$

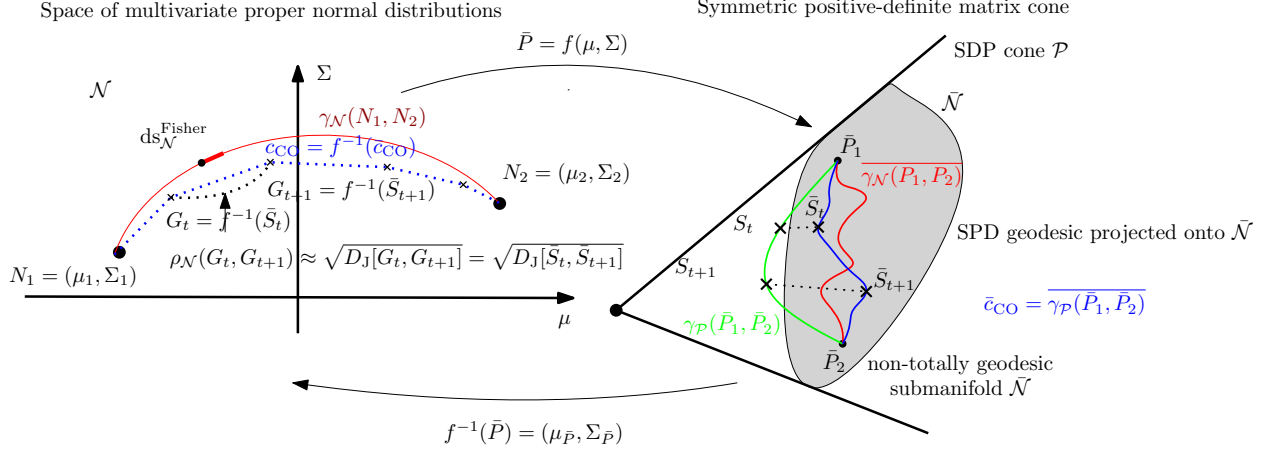


Figure 8: Illustration of the approximation of the Fisher-Rao distance between two multivariate normals N_1 and N_2 (red geodesic length $\gamma_{\mathcal{N}}(N_1, N_2)$) by discretizing curve $\bar{c}_{\text{CO}} \in \bar{\mathcal{N}}$ or equivalently curve $c_{\text{CO}} \in \mathcal{N}$.

Indeed, using the inverse matrix

$$f(\mu, \Sigma)^{-1} = \begin{bmatrix} \Sigma^{-1} & -\Sigma^{-1}\mu \\ -\mu^\top \Sigma^{-1} & 1 + \mu^\top \Sigma^{-1}\mu \end{bmatrix},$$

we have

$$\begin{aligned} \text{tr}(\bar{P}_2^{-1}\bar{P}_1) &= \text{tr} \left(\begin{bmatrix} \Sigma_2^{-1} & -\Sigma_2^{-1}\mu_2 \\ -\mu_2^\top \Sigma_2^{-1} & 1 + \mu_2^\top \Sigma_2^{-1}\mu_2 \end{bmatrix} \begin{bmatrix} \Sigma_1 + \mu_1\mu_1^\top & \mu_1 \\ \mu_1^\top & 1 \end{bmatrix} \right), \\ &= 1 + \text{tr}(\Sigma_2^{-1}\Sigma_1 + \Delta_\mu^\top \Sigma_2^{-1}\Delta_\mu). \end{aligned}$$

Thus even if the dimension of the sample spaces of $p_{\mu, \Sigma}$ and $q_{\bar{P}=f(\mu, \Sigma)}$ differs by one, we get the same KLD by Calvo and Oller's isometric mapping f . \square

This property holds for the KLD/Jeffreys divergence but not for all f -divergences [4] I_f in general (e.g., it fails for the Hellinger divergence).

Figure 9 shows the various geodesics and curves used to approximate the Fisher-Rao distance with the Fisher metric shown using Tissot indicatrices.

Note that the introduction of parameter β is related to the foliation of the SPD cone \mathcal{P} by $\{f_\beta(\mathcal{N}) : \beta > 0\}$: $\mathcal{P}(d+1) = \mathbb{R}_{>0} \times f_\beta(\mathcal{N})$. See Figure 6. Thus we may define how good the projected C&O curve is to the Fisher-Rao geodesic by measuring the average distance between points on $\gamma_{\mathcal{P}}(\bar{P}_1, \bar{P}_2; t)$ and their projections $\overline{\gamma_{\mathcal{P}}(\bar{P}_1, \bar{P}_2; t)}^\perp$ onto $\bar{\mathcal{N}}$:

$$\delta^{\text{CO}}(P_1, P_2) = \int_0^1 \rho_{\mathcal{P}}(\gamma_{\mathcal{P}}(\bar{P}_1, \bar{P}_2; t), \overline{\gamma_{\mathcal{P}}(\bar{P}_1, \bar{P}_2; t)}^\perp) dt.$$

In practice, we evaluate this integral at the sampling points S_t :

$$\delta^{\text{CO}}(P_1, P_2) \approx \delta_T^{\text{CO}}(P_1, P_2) = \frac{1}{T} \sum_{i=1}^T \rho_{\mathcal{P}}(S_t, \bar{S}_t), \quad (23)$$

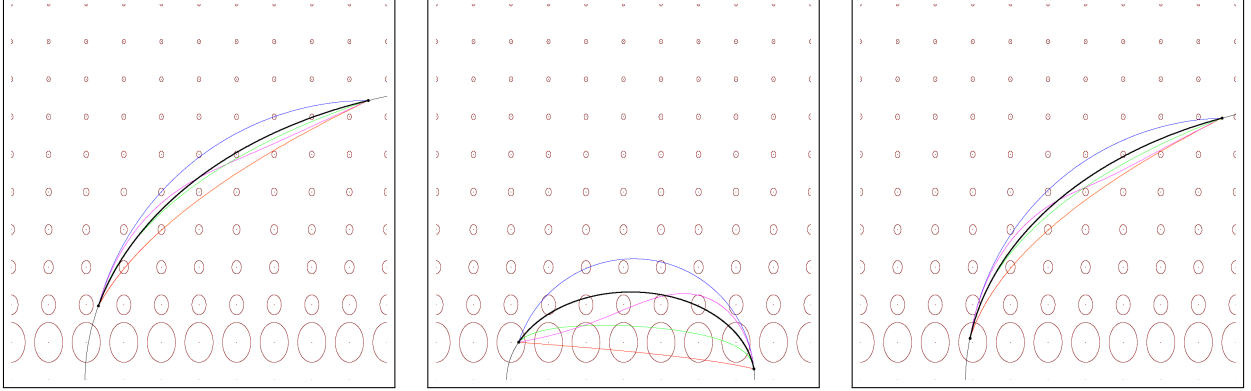


Figure 9: Geodesics and curves used to approximate the Fisher-Rao distance with the Fisher metric shown using Tissot's indicatrices: exponential geodesic (red), mixture geodesic (blue), mid exponential-mixture curve (purple), projected CO curve (green) and target Fisher-Rao geodesic (black). (Visualization in the parameter space of normal distributions.)

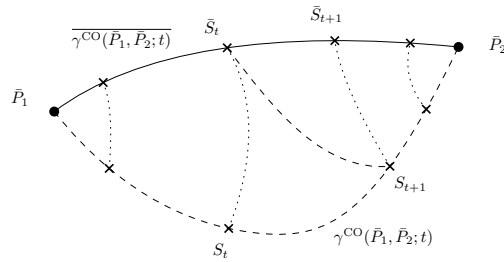


Figure 10: Bounding $\rho_{\mathcal{N}}(\bar{S}_t, \bar{S}_{t+1})$ using the triangular inequality of $\rho_{\mathcal{P}}$ in the SPD cone $\mathcal{P}(d+1)$.

where $S_t = \gamma_{\mathcal{P}}(\bar{P}_1, \bar{P}_2; t)$ and $\bar{S}_t = \gamma_{\mathcal{P}}(\bar{P}_1, \bar{P}_2; t)^\perp$. We checked experimentally (see Section 3.3) that for close by normals N_1 and N_2 , we have $\delta^{\text{CO}}(\bar{N}_1, \bar{N}_2)$ small, and that when N_1 gets further separated from N_2 , the average projection error $\delta^{\text{CO}}(\bar{N}_1, \bar{N}_2)$ increases. Thus $\delta_T^{\text{CO}}(P_1, P_2)$ is a good measure of the precision of our Fisher-Rao distance approximation.

Property 5 We have $\rho_{\bar{\mathcal{N}}}(\bar{S}_t, \bar{S}_{t+1}) \leq \rho_{\mathcal{P}}(\bar{S}_t, S_t) + \rho_{\mathcal{P}}(S_t, S_{t+1}) + \rho_{\mathcal{P}}(S_{t+1}, \bar{S}_{t+1})$.

Proof: The proof consists in applying twice the triangle inequality of metric distance $\rho_{\mathcal{P}}$:

$$\begin{aligned} \rho_{\bar{\mathcal{N}}}(\bar{S}_t, \bar{S}_{t+1}) &\leq \rho_{\mathcal{P}}(\bar{S}_t, S_{t+1}) + \rho_{\mathcal{P}}(S_{t+1}, \bar{S}_{t+1}), \\ &\leq \rho_{\mathcal{P}}(\bar{S}_t, S_t) + \rho_{\mathcal{P}}(S_t, S_{t+1}) + \rho_{\mathcal{P}}(S_{t+1}, \bar{S}_{t+1}). \end{aligned}$$

See Figure 10. □

Property 6 We have $\rho_{\mathcal{N}}(N_1, N_2) \leq \rho_{\bar{\mathcal{N}}}^{\text{CO}}(N_1, N_2) \leq \rho_{\mathcal{N}}(N_1, N_2) + 2\delta_T^{\text{CO}}(\bar{P}_1, \bar{P}_2)$.

Proof: At infinitesimal scale, we have

$$ds_{\mathcal{N}}(\bar{S}_t) \leq ds_{\mathcal{P}}(S_t) + 2\rho_{\mathcal{P}}(S_t, \bar{S}_t).$$

Taking the integral, we get

$$\rho_{\mathcal{N}}(N_1, N_2) \leq \rho_{\mathcal{P}}(\bar{P}_1, \bar{P}_2) + 2\delta_T^{\text{CO}}(\bar{P}_1, \bar{P}_2)$$

Since $\rho_{\mathcal{P}}(P_1, P_2) \leq \rho_{\mathcal{N}}(N_1, N_2)$, we have

$$\rho_{\mathcal{N}}(N_1, N_2) \leq \rho_{\bar{\mathcal{N}}}^{\text{CO}}(N_1, N_2) \leq \rho_{\mathcal{N}}(N_1, N_2) + 2\delta_T^{\text{CO}}(\bar{P}_1, \bar{P}_2).$$

□

Example 1 Let us consider Example 1 of [76] (p. 11):

$$N_1 = \left(\left[\begin{array}{c} -1 \\ 0 \end{array} \right], \Sigma \right), \quad N_2 = \left(\left[\begin{array}{c} 6 \\ 3 \end{array} \right], \Sigma \right), \quad \Sigma = \left[\begin{array}{cc} 1.1 & 0.9 \\ 0.9 & 1.1 \end{array} \right].$$

The Fisher-Rao distance is evaluated numerically in [76] as 5.00648. We have the lower bound $\rho_{\bar{\mathcal{N}}}^{\text{CO}}(N_1, N_2) = 4.20447$, and the Mahalanobis distance 8.06226 upper bounds the Fisher-Rao distance (not totally geodesic submanifold \mathcal{N}_Σ). Our projected $\mathcal{C}\mathcal{E}\mathcal{O}$ curve discretized with $T = 1000$ yields an approximation $\tilde{\rho}_{\bar{\mathcal{N}}}^{\text{CO}}(N_1, N_2) = 5.31667$. The average projection distance $\rho_{\mathcal{P}}(S_t, \bar{S}_t)$ is $\delta_T^{\text{CO}}(N_1, N_2) = 0.61791$, and the maximum projected distance is 1.00685. We check that

$$5.00648 \approx \rho_{\mathcal{N}}(N_1, N_2) \leq \tilde{\rho}_{\bar{\mathcal{N}}}^{\text{CO}}(N_1, N_2) \approx 5.31667 \leq \rho_{\mathcal{N}}(N_1, N_2) + 2\delta_T^{\text{CO}}(\bar{P}_1, \bar{P}_2) \approx 5.44028.$$

The Killing distance obtained for $\kappa_{\text{Killing}} = 2$ is $\rho_{\text{Killing}}(N_1, N_2) \approx 6.82028$. Notice that geodesic shooting is time consuming compared to our approximation technique.

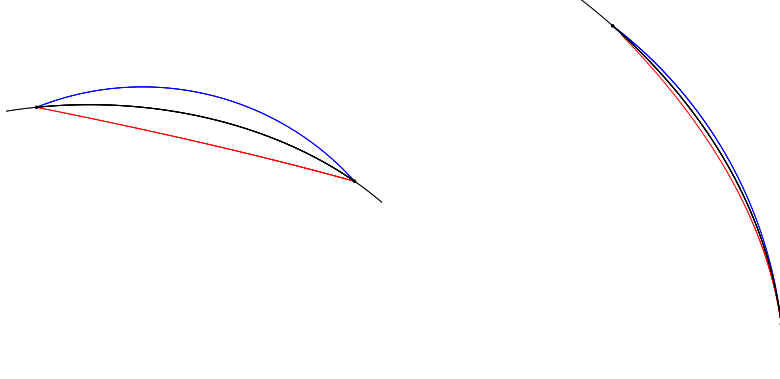


Figure 11: The full Fisher-Rao geodesic is shown in grey with the geodesic arc linking two univariate normal distributions shown in black. The exponential geodesics are shown in red and are below the Fisher-Rao geodesic. The mixture geodesics are shown in blue and are above the Fisher-Rao geodesic.

3.3 Some experiments

The KLD D_{KL} and Jeffreys divergence D_J , the Fisher-Rao distance $\rho_{\mathcal{N}}$ and the Calvo & Oller distance ρ_{CO} are all invariant under the congruence action of the affine group $\text{Aff}(d) = \mathbb{R}^d \rtimes \text{GL}(d)$ with group operation

$$(a_1, A_1)(a_2, A_2) = (a_1 + A_1 a_2, A_1 A_2).$$

Let $(A, a) \in \text{Aff}(d)$, and define the action on the normal space \mathcal{N} as follows:

$$(A, a).N(\mu, \Sigma) = N(A^\top \mu + a, A \Sigma A^\top).$$

Then we have $\rho_{\mathcal{N}}((A, a).N_1, (A, a).N_2) = \rho_{\mathcal{N}}(N_1, N_2)$, $\rho_{\text{CO}}((A, a).N_1, (A, a).N_2) = \rho_{\text{CO}}(N_1, N_2)$ and $D_{\text{KL}}[(A, a).N_1 : (A, a).N_2] = D_{\text{KL}}[N_1 : N_2]$. This invariance extends to our approximations $\tilde{\rho}_{\mathcal{N}}^c$ (see Eq. 22).

Since we have

$$\tilde{\rho}_{\mathcal{N}}^c(N_1, N_2) \approx \rho_{\mathcal{N}}(N_1, N_2) \geq \rho_{\text{CO}}(N_1, N_2),$$

the ratio $\kappa_c = \frac{\tilde{\rho}_{\mathcal{N}}^c}{\rho_{\text{CO}}} \geq \kappa = \frac{\tilde{\rho}_{\mathcal{N}}^c}{\rho_{\mathcal{N}}}$ gives an upper bound on the approximation factor of $\tilde{\rho}_{\mathcal{N}}^c$ compared to the true Fisher-Rao distance $\rho_{\mathcal{N}}$:

$$\kappa_c \rho_{\mathcal{N}}(N_1, N_2) \geq \kappa \rho_{\mathcal{N}}(N_1, N_2) \geq \tilde{\rho}_{\mathcal{N}}^c(N_1, N_2) \approx \rho_{\mathcal{N}}(N_1, N_2) \geq \rho_{\text{CO}}(N_1, N_2).$$

Let us now report some numerical experiments of our approximated Fisher-Rao distances $\tilde{\rho}_{\mathcal{N}}^x$ with $x \in \{l, m, e, \text{em}, \text{CO}\}$. When normal distributions are in 1D we can exactly plot the Fisher-Rao geodesics and locate the other geodesics/curves with respect to the Fisher-Rao geodesics (Figure 11). Although that dissimilarity $\tilde{\rho}_{\mathcal{N}}$ is positive-definite, it does not satisfy the triangular inequality of metric distances (e.g., Riemannian distances $\rho_{\mathcal{N}}$ and ρ_{CO}).

First, we draw multivariate normals by sampling means $\mu \sim \text{Unif}(0, 1)$ and sample covariance matrices Σ as follows: We draw a lower triangular matrix L with entries L_{ij} iid sampled from $\text{Unif}(0, 1)$, and take $\Sigma = LL^\top$. We use $T = 1000$ samples on curves and repeat the experiment 1000 times to gather average statistics on κ_c 's of curves. Results are summarized in Table 1.

Table 1: First set of experiments demonstrates the advantage of the $c_{\text{CO}}(t)$ curve.

d	κ_{CO}	κ_l	κ_e	κ_m	κ_{em}
1	1.0025	1.0414	1.1521	1.0236	1.0154
2	1.0167	1.0841	1.1923	1.0631	1.0416
3	1.0182	1.8997	2.6072	1.9965	1.07988
4	1.0207	2.0793	1.8080	2.1687	1.1873
5	1.0324	4.1207	12.3804	5.6170	4.2349

Table 2: Comparing our Fisher-Rao approximation with the Calvo & Oller lower bound and the Strapasson et al. upper bound.

d	$\rho_{\text{CO}}(N_1, N_2)$	$\tilde{\rho}^{\text{cCO}}(N_1, N_2)$	$U(N_1, N_2)$
1	1.7563	1.8020	3.1654
2	3.2213	3.3194	6.012
3	4.6022	4.7642	8.7204
4	5.9517	6.1927	11.3990
5	7.156	7.3866	13.8774

For that scenario that the C&O curve (either $\bar{c}_{\text{CO}} \in \bar{\mathcal{N}}$ or $c_{\text{CO}} \in \mathcal{N}$) performs best compared to the linear interpolation curves with respect to source parameter (l), mixture geodesic (m), exponential geodesic (e), or exponential-mixture mid curve (em). Let us point out that we sample $\gamma_{\mathcal{P}}(\bar{P}_1, \bar{P}_2; \frac{i}{T})$ for $i \in \{0, \dots, T\}$.

Strapasson, Porto and Costa [87] (SPC) reported the following upper bound on the Fisher-Rao distance between multivariate normals:

$$\rho_{\text{CO}}(N_1, N_2) \leq \rho_{\mathcal{N}}(N_1, N_2) \leq U_{\text{SPC}}(N_1, N_2) = \sqrt{2 \sum_{i=1}^d \log^2 \left(\frac{\sqrt{(1 + D_{ii})^2 + \mu_i^2} + \sqrt{(1 - D_{ii})^2 + \mu_i^2}}{\sqrt{(1 + D_{ii})^2 + \mu_i^2} - \sqrt{(1 - D_{ii})^2 + \mu_i^2}} \right)}, \quad (24)$$

where $\Sigma = \Sigma_1^{-\frac{1}{2}} \Sigma_2 \Sigma_1^{-\frac{1}{2}}$, $\Sigma = \Omega D \Omega^\top$ is the eigen decomposition, and $\mu = \Omega^\top \Sigma_1^{-\frac{1}{2}} (\mu_2 - \mu_1)$. This upper bound performs better when the normals are well-separated and worse than the $\sqrt{D_J}$ -upper bound when the normals are close to each others.

Let us compare $\rho_{\text{CO}}(N_1, N_2)$ with $\rho_{\mathcal{N}}(N_1, N_2) \approx \tilde{\rho}^{\text{cCO}}(N_1, N_2)$ and the upper bound $U(N_1, N_2)$ by averaging over 1000 trials with N_1 and N_2 chosen randomly as before and $T = 1000$. We have $\rho_{\text{CO}}(N_1, N_2) \leq \rho_{\mathcal{N}}(N_1, N_2) \approx \tilde{\rho}^{\text{cCO}}(N_1, N_2) \leq U(N_1, N_2)$. Table 2 shows that our Fisher-Rao approximation is close to the lower bound (and hence to the underlying true Fisher-Rao distance) and that the upper bound is about twice the lower bound for that particular scenario.

The Fisher-Rao geodesics $\gamma_{\mathcal{N}}^{\text{FR}}(N_1, N_2)$ on the Fisher-Rao univariate normal manifolds are either vertical line segments when $\mu_1 = \mu_2$, or semi-circle with origin on the x -axis and x -axis stretched by $\sqrt{2}$ [90]:

$$\gamma_{\mathcal{N}}^{\text{FR}}(\mu_1, \sigma_1; \mu_2, \sigma_2) = \begin{cases} (\mu, (1-t)\sigma_1 + t\sigma_2), & \mu_1 = \mu_2 = \mu \\ (\sqrt{2}(c + r \cos t), r \sin t), t \in [\min\{\theta_1, \theta_2\}, \max\{\theta_1, \theta_2\}], & \mu_1 \neq \mu_2, \end{cases},$$

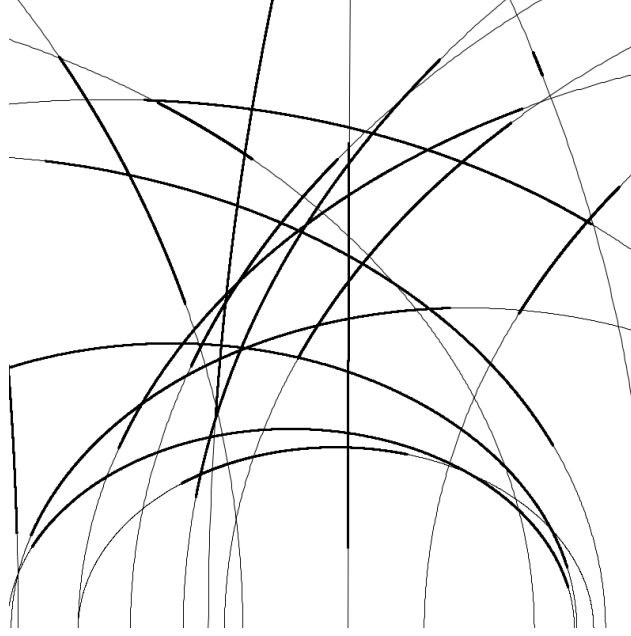


Figure 12: Visualizing some Fisher-Rao geodesics of univariate normal distributions on the Poincaré upper plane (semi-circles with origin on the x -axis and stretched by $\sqrt{2}$ on the x -axis). Full geodesics plotted with thin style and geodesic arcs plotted with thick style.

where

$$c = \frac{\frac{1}{2}(\mu_2^2 - \mu_1^2) + \sigma_2^2 - \sigma_1^2}{\sqrt{2}(\mu_1 - \mu_2)}, \quad r = \sqrt{\left(\frac{\mu_i}{\sqrt{2}} - c\right)^2 + \sigma_i^2}, i \in \{1, 2\},$$

and

$$\theta_i = \arctan\left(\frac{\sigma_i}{\frac{\mu_i}{\sqrt{2}} - c}\right), i \in \{1, 2\},$$

provided that $\theta_i \geq 0$ for $i \in \{1, 2\}$ (otherwise, we let $\theta_i \leftarrow \theta_i + \pi$). Figure 12 displays some geodesics on the Fisher-Rao univariate normal manifold. Figure 13 displays the considered geodesics and curves in the stretched Poincaré upper plane of univariate normal distributions (x -axis is stretched by $\sqrt{2}$) (in 1D for illustration purpose).

Second, since the distances are invariant under the action of the affine group, we can set wlog. $N_1 = (0, I)$ (standard normal distribution) and let $N_2 = \text{diag}(u_1, \dots, u_d)$ where $u_i \sim \text{Unif}(0, a)$. As normals N_1 and N_2 separate to each others, we notice experimentally that the performance of the c_{CO} curve degrades in the second experiment with $a = 5$ (see Table 3): Indeed, the mixture geodesic works experimentally better than the C&O curve when $d \geq 11$.

Figure 14 and Figure 15 display the various curves considered for approximating the Fisher-Rao distance between bivariate normal distributions: For a curve $c(t)$, we visualize its corresponding bivariate normal distributions $(\mu_{c(t)}, \Sigma_{c(t)})$ at several increment steps $t \in [0, 1]$ by plotting the ellipsoid

$$E_{c(t)} = \mu_{c(t)} + \left\{ L^\top x, x = (\cos \theta, \sin \theta), \theta \in [0, 2\pi) \right\},$$

where $\Sigma_{c(t)} = L_{c(t)} L_{c(t)}^\top$.

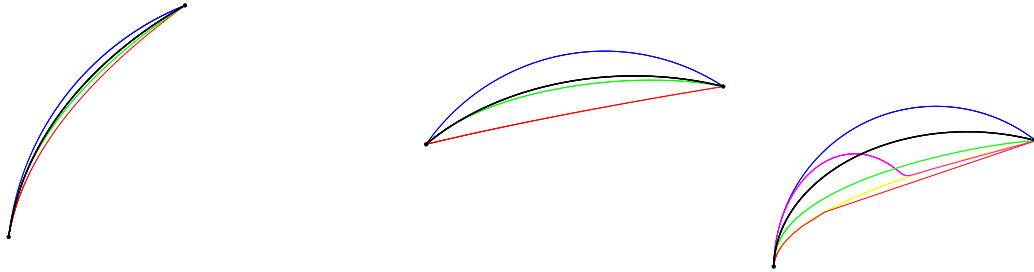


Figure 13: Visualizing the geodesics and curves in the Poincaré upper plane with x -axis stretched by $\sqrt{2}$: (a) and (b): Fisher-Rao geodesic (black), our projected Calvo & Oller curve (green), the mixture geodesic (blue), and the exponential geodesic (red). (c): interpolation in ordinary parameterization λ (yellow), mid mixture-exponential curve (purple). The range is $[-1, 1] \times (0, 2]$.

Table 3: Second set of experiments shows limitations of the $c_{CO}(t)$ curve.

d	κ_{CO}	κ_l	κ_e	κ_m
1	1.0569	1.1405	1.139	1.0734
5	1.1599	1.4696	1.5201	1.1819
10	1.2180	1.6963	1.7887	1.2184
11	1.2260	1.7333	1.8285	1.2235
12	1.2301	1.7568	1.8539	1.2282
15	1.2484	1.8403	1.9557	1.2367
20	1.2707	1.9519	2.0851	1.2466

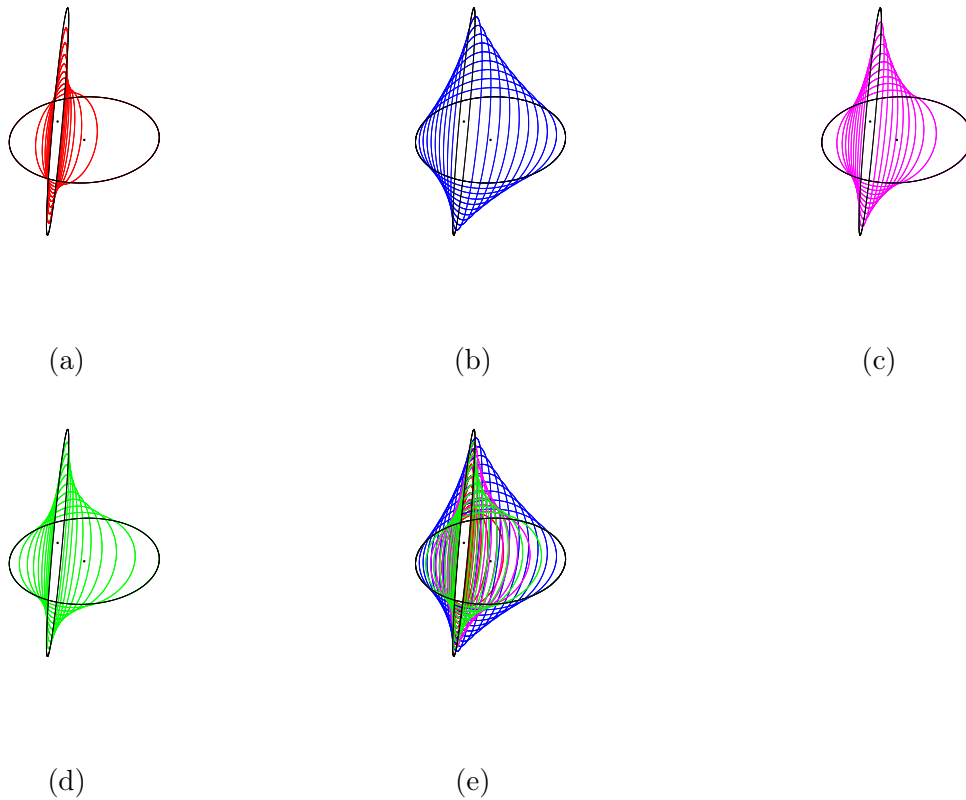


Figure 14: Visualizing at discrete positions (10 increment steps between 0 and 1) some curves used to approximate the Fisher-Rao distance between two bivariate normal distributions: (a) exponential geodesic $c^e = \gamma_{\mathcal{N}}^e$ (red), (b) mixture geodesic $c^m = \gamma_{\mathcal{N}}^m$ (blue), (c) mid mixture-exponential curve c^{em} (purple), (d) projected Calvo & Oller curve c^{CO} (green), and (e) All superposed curves at once. Visualization in the 2D sample space of bivariate normal distributions because bivariate normals are modeled as a $m = 5$ dimensional point on the Fisher-Rao manifold \mathcal{M} .

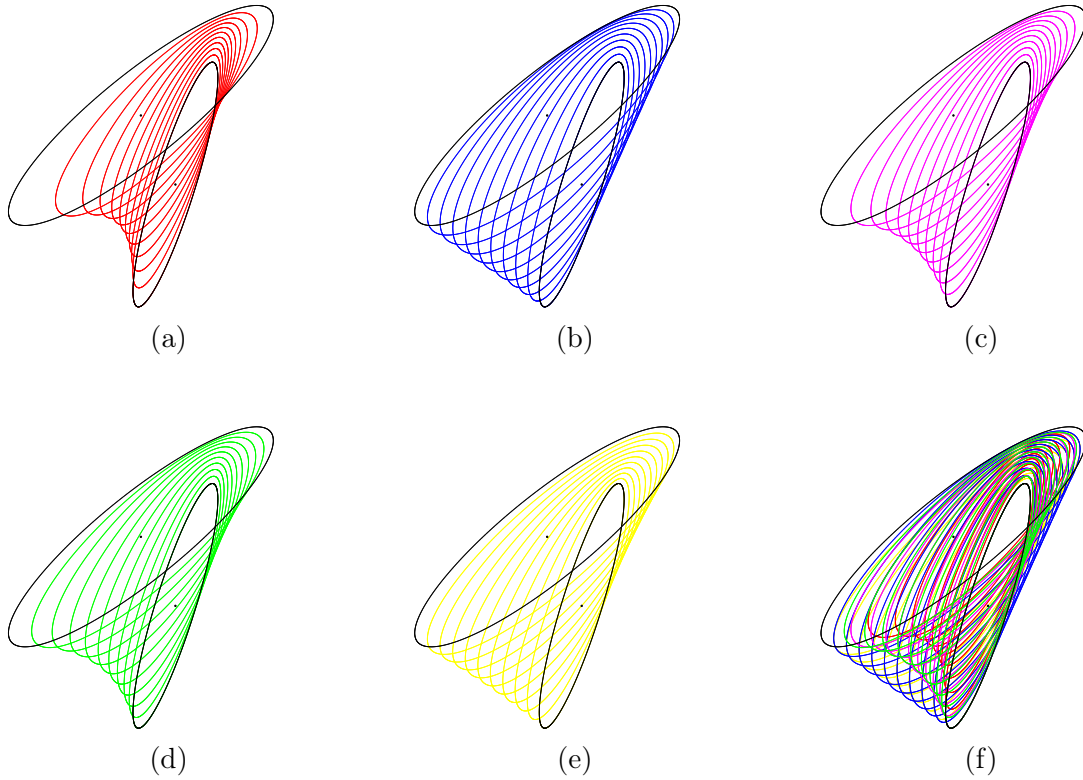


Figure 15: Visualizing at discrete positions (10 increment steps between 0 and 1) some curves used to approximate the Fisher-Rao distance between two bivariate normal distributions: (a) exponential geodesic $c^e = \gamma_{\mathcal{N}}^e$ (red), (b) mixture geodesic $c^m = \gamma_{\mathcal{N}}^m$ (blue), (c) mid mixture-exponential curve c^{em} (purple), (d) projected Calvo & Oller curve c^{CO} (green), (e) c^λ : ordinary linear interpolation in λ (yellow), and (f) All superposed curves at once.

Example 2 Let us report some numerical results for bivariate normals with $T = 1000$:

- We use the following example of Han and Park [40] (Eq. 26):

$$N_1 = \left(\begin{bmatrix} 0 \\ 0 \end{bmatrix}, \begin{bmatrix} 1 & 0 \\ 0 & 0.1 \end{bmatrix} \right), \quad N_2 = \left(\begin{bmatrix} 1 \\ 1 \end{bmatrix}, \begin{bmatrix} 0.1 & 0 \\ 0 & 1 \end{bmatrix} \right).$$

Their geodesic shooting algorithm [40] evaluates the Fisher-Rao distance to $\rho_{\mathcal{N}}(N_1, N_2) \approx \mathbf{3.1329}$ (precision 10^{-5}).

We get:

- Calvo & Oller lower bound: $\rho_{\text{CO}}(N_1, N_2) \approx \mathbf{3.0470}$,
- Upper bound using Eq. 11: 7.92179,
- SPC upper bound (Eq. 24): $U_{\text{SPC}}(N_1, N_2) \approx 5.4302$,
- $\sqrt{D_J}$ upper bound: $U_{\sqrt{J}}(N_1, N_2) \approx \mathbf{4.3704}$,
- $\tilde{\rho}_{\mathcal{N}}^{\lambda}(N_1, N_2) \approx 3.4496$,
- $\tilde{\rho}_{\mathcal{N}}^m(N_1, N_2) \approx 3.5775$,
- $\tilde{\rho}_{\mathcal{N}}^e(N_1, N_2) \approx 3.7314$,
- $\tilde{\rho}_{\mathcal{N}}^{\text{em}}(N_1, N_2) \approx 3.1672$,
- $\tilde{\rho}_{\mathcal{N}}^{\text{CO}}(N_1, N_2) \approx \mathbf{3.1391}$.

In that setting, the $\sqrt{D_J}$ upper bound is better than the upper bound of Eq. 24, and the projected Calvo & Oller geodesic yields the best approximation of the Fisher-Rao distance (Figure 16) with an absolute error of 0.0062 (about 0.2% relative error). When $T = 10$, we have $\tilde{\rho}_{\mathcal{N}}^{\text{CO}}(N_1, N_2) \approx 3.1530$, when $T = 100$, we get $\tilde{\rho}_{\mathcal{N}}^{\text{CO}}(N_1, N_2) \approx 3.1136$, and when $T = 500$ we obtain $\tilde{\rho}_{\mathcal{N}}^{\text{CO}}(N_1, N_2) \approx 3.1362$ (which is better than the approximation obtained for $T = 1000$). Figure 17 shows the fluctuations of the approximation of the Fisher-Rao distance by the projected C&O curve when T ranges from 3 to 100.

- Bivariate normal $N_1 = (0, I)$ and bivariate normal $N_2 = (\mu_2, \Sigma_2)$ with $\mu_2 = [1 \ 0]^{\top}$ and $\Sigma_2 = \begin{bmatrix} 1 & -1 \\ -1 & 2 \end{bmatrix}$. We get

- Calvo & Oller lower bound: 1.4498
- Upper bound of Eq. 24: 2.6072
- $\sqrt{D_J}$ upper bound: 1.5811
- $\tilde{\rho}^{\lambda}$: 1.5068
- $\tilde{\rho}^m$: 1.5320
- $\tilde{\rho}^e$: 1.5456
- $\tilde{\rho}^{\text{em}}$: 1.4681
- $\tilde{\rho}^{\text{co}}$: 1.4673

- Bivariate normal $N_1 = (0, I)$ and bivariate normal $N_2 = (\mu_2, \Sigma_2)$ with $\mu_2 = [5 \ 0]^{\top}$ and $\Sigma_2 = \begin{bmatrix} 1 & -1 \\ -1 & 2 \end{bmatrix}$. We get:

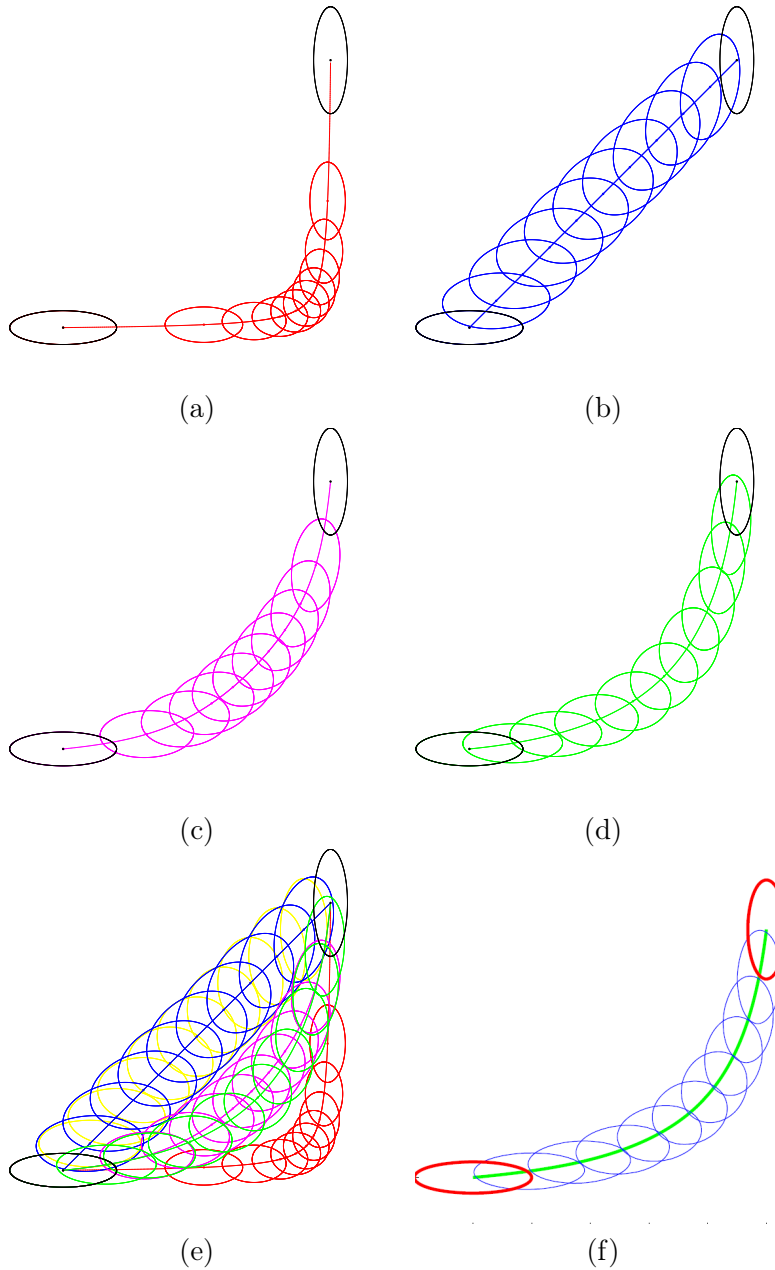


Figure 16: Comparison of our approximation curves with the Fisher-Rao geodesic (f) obtained by geodesic shooting (Figure 5 of [40]). Exponential (a) and mixture (b) geodesics with the mid exponential-mixture curve (c), and the projected C&O curve (d). Superposed curves (e) and comparison with geodesic shooting (Figure 5 of [40]). Beware that color coding are not related between (a) and (b), and scale for depicting ellipsoids are different.

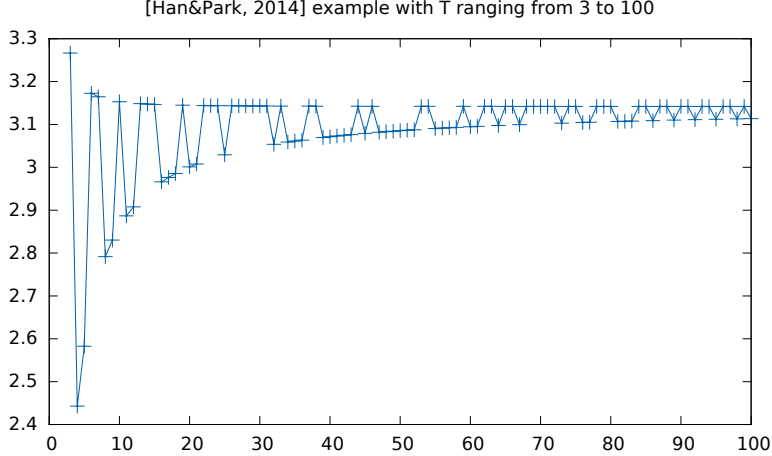


Figure 17: Approximating of the Fisher-Rao distance obtained by using the projected C&O curve when T ranges from 3 to 100.

- Calvo & Oller lower bound: 3.6852
- Upper bound of Eq. 24: 6.0392
- $\sqrt{D_J}$ upper bound: 6.2048
- $\tilde{\rho}^\lambda$: 5.7319
- $\tilde{\rho}^m$: 4.4039
- $\tilde{\rho}^e$: 5.9205
- $\tilde{\rho}^{\text{em}}$: 4.2901
- $\tilde{\rho}^{\text{co}}$: 4.3786

4 Approximating the smallest enclosing Fisher-Rao ball of MVNs

We may use these closed-form distance $\rho_{\text{CO}}(N, N')$ between N and N' to compute an approximation (of the center) of the smallest enclosing Fisher-Rao ball $B^* = \text{ball}(C^*, r^*)$ of a set $\mathcal{G} = \{N_1 = (\mu_1, \Sigma_1), \dots, N_n = (\mu_n, \Sigma_n)\}$ of n d -variate normal distributions:

$$C^* = \arg \min_{C \in \mathcal{N}} \max_{i \in \{1, \dots, n\}} \rho_{\mathcal{N}}(C, N_i)$$

where $\text{ball}(C, r) = \{N \in \mathcal{N} : \rho_{\mathcal{N}}(C, N) \leq r\}$.

The method proceeds as follows:

- First, we convert MVN set \mathcal{G} into the equivalent set of $(d + 1)$ -dimensional SPD matrices $\bar{\mathcal{G}} = \{\bar{P}_i = f(N_i)\}$ using the C&O embedding. We relax the problem of approximating the circumcenter C^* of the smallest enclosing Fisher-Rao ball by

$$P^* = \arg \min_{P \in \mathbb{P}(d+1)} \max_{i \in \{1, \dots, n\}} \rho_{\text{CO}}(P, \bar{P}_i).$$

- Second we approximate the center of the smallest enclosing Riemannian ball of $\bar{\mathcal{G}}$ using the iterative smallest enclosing Riemannian ball algorithm in [5] with say $T = 1000$ iterations. Let $\tilde{P} \in \mathbb{P}(d+1)$ denote this approximation center: $P_T = \text{RieSEB}_{\text{SPD}}(\bar{\mathcal{G}}, T)$.
- Finally, we project back P_T onto $\bar{\mathcal{N}}$: $\bar{P}_T = \text{proj}_{\bar{\mathcal{N}}}(P_T)$. We return \bar{P}_T as the approximation of C^* .

Algorithm [5] $\text{RieSEB}_{\text{SPD}}(\{P_1, \dots, P_n\}, T)$ is described for a set of SPD matrices $\{P_1, \dots, P_n\}$ as follows:

- Let $C_1 \leftarrow P_1$
- For $t = 1$ to T
 - Compute the index of the SPD matrix which is farthest to current circumcenter C_t :

$$f_t = \arg \max_{i \in \{1, \dots, n\}} \rho_{\text{SPD}}(C_t, P_i)$$

- Update the circumcenter by walking along the geodesic linking C_t to P_{f_t} :

$$C_{t+1} = \gamma_{\text{SPD}} \left(C_t, P_{f_t}; \frac{1}{t+1} \right) = C_t^{\frac{1}{2}} (C_t^{-\frac{1}{2}} P_{f_t} C_t^{-\frac{1}{2}})^{\frac{1}{t+1}} C_t^{\frac{1}{2}}$$

- Return C_T

Convergence of the algorithm $\text{RieSEB}_{\text{SPD}}$ follows from the fact that the SPD trace manifold is a Hadamard manifold (with negative sectional curvatures). See [5] for a proof of convergence (and [66] for a convergence proof of the similar algorithm in hyperbolic geometry).

The SPD distance $\rho_{\mathcal{P}}(C_T, \bar{C}_T)$ provides an indication of the quality of the approximation. Figure 18 shows the result of implementing this heuristic.

Let us notice that when all MVNs share the same covariance matrix Σ , we have from Eq. 14 or Eq. 18 that $\rho_{\mathcal{N}}(\mu_1, \Sigma), N(\mu_2, \Sigma)$ and $\rho_{\text{CO}}(N(\mu_1, \Sigma), N(\mu_2, \Sigma))$ are strictly increasing function of their Mahalanobis distance. Using the the Cholesky decomposition $\Sigma^{-1} = LL^\top$, we deduce that the smallest Fisher-Rao enclosing ball coincides with the smallest Calvo & Oller enclosing ball, and the circumcenter of that ball can be found as an ordinary Euclidean circumcenter [95] (Figure 18(b)). Note that in 1D, we can find the exact smallest enclosing Fisher-Rao ball as an equivalent smallest enclosing ball in hyperbolic geometry [67].

Furthermore, we may extend the computation of the approximated circumcenter to k -center clustering [37] of n multivariate normal distributions. Since the circumcenter of the clusters are approximated and not exact, we extend straightforwardly the variational approach of k -means described in [1] to k -center clustering. An application of k -center clustering of MVNs is to simplify a Gaussian mixture model [76] (GMM).

Similarly, we can consider other Riemannian distances with closed form formula between MVNs like the Killing distance in the symmetric space [53] or the Siegel-based distance proposed in Appendix B.

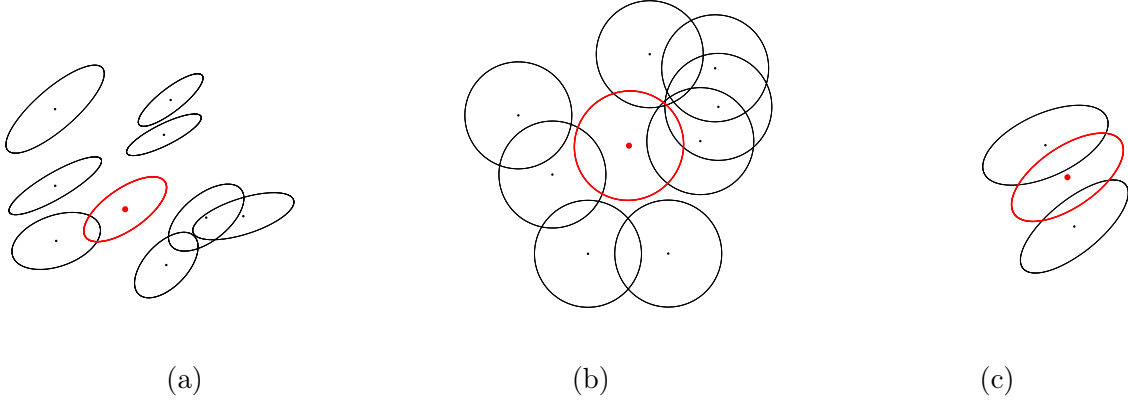


Figure 18: Approximation of the smallest enclosing Riemannian ball of a set of n bivariate normals $N_i = N(\mu_i, \Sigma_i)$ with respect to C&O distance ρ_{CO} (the approximate circumcenter \bar{C}_T is depicted as a red ellipse): (a) $n = 8$ with different covariance matrices, (b) $n = 8$ with identical covariance matrices amount to a smallest enclosing ball of a set of n points $\{\mu_i\}$, (c) $n = 2$ displays the midpoint of the C&O geodesic visualized as an equivalent bivariate normal distribution in the sample space.

5 Some information-geometric properties of the C&O embedding

In information geometry [4], the manifold \mathcal{N} admits a dual structure $(\mathcal{N}, g_{\mathcal{N}}^{\text{Fisher}}, \nabla_{\mathcal{N}}^e, \nabla_{\mathcal{N}}^m)$ when equipped with the exponential connection $\nabla_{\mathcal{N}}^e$ and the mixture connection $\nabla_{\mathcal{N}}^m$. The connections $\nabla_{\mathcal{N}}^e$ and $\nabla_{\mathcal{N}}^m$ are said dual since $\frac{\nabla_{\mathcal{N}}^e + \nabla_{\mathcal{N}}^m}{2} = \bar{\nabla}_{\mathcal{N}}$, the Levi-Civita connection induced by $g_{\mathcal{N}}^{\text{Fisher}}$. Furthermore, by viewing \mathcal{N} as an exponential family $\{p_{\theta}\}$ with natural parameter $\theta = (\theta_v, \theta_M)$ (using the sufficient statistics [63] $(x, -xx^{\top})$), and taking the convex log-normalizer function $F_{\mathcal{N}}(\theta)$ of the normals, we can build a dually flat space [4] where the canonical divergence amounts to a Bregman divergence which coincides with the reverse Kullback-Leibler divergence [72, 96] (KLD). The Legendre duality

$$F^*(\eta) = \langle \nabla F(\theta), \eta \rangle - F(\nabla F(\theta))$$

(with $\langle (v_1, M_1), (v_2, M_2) \rangle = \text{tr}(v_1 v_2^{\top} + M_1 M_2^{\top}) = v_1 \cdot v_2 + \text{tr}(M_1 M_2^{\top})$) yields: $\theta = (\theta_v, \theta_M) = (\Sigma^{-1} \mu, \frac{1}{2} \Sigma^{-1})$,

$$F_{\mathcal{N}}(\theta) = \frac{1}{2} \left(d \log \pi - \log |\theta_M| + \frac{1}{2} \theta_v^{\top} \theta_M^{-1} \theta_v \right),$$

$$\eta = (\eta_v, \eta_M) = \nabla F_{\mathcal{N}}(\theta) = \left(\frac{1}{2} \theta_M^{-1} \theta_v, \theta_M^{-1} \right),$$

$$F_{\mathcal{N}}^*(\eta) = -\frac{1}{2} \left(\log(1 + \eta_v^{\top} \eta_M^{-1} \eta_v) + \log |-\eta_M| + d(\log 2\pi e) \right),$$

and we have

$$B_{F_{\mathcal{N}}}(\theta_1, \theta_2) = D_{\text{KL}}^*(p_{\lambda_1} : p_{\lambda_2}) = D_{\text{KL}}(p_{\lambda_2} : p_{\lambda_1}) = B_{F_{\mathcal{N}}^*}(\eta_2 : \eta_1),$$

where $D_{\text{KL}}^*[p : q] = D_{\text{KL}}[q : p]$ is the reverse KLD.

In a dually flat space, we can express the canonical divergence as a Fenchel-Young divergence using the mixed coordinate systems $B_{F_{\mathcal{N}}}(\theta_1 : \theta_2) = Y_{F_{\mathcal{N}}}(\theta_1 : \eta_2)$ where $\eta_i = \nabla F_{\mathcal{N}}(\theta_i)$ and

$$Y_{F_{\mathcal{N}}}(\theta_1 : \eta_2) := F_{\mathcal{N}}(\theta_1) + F_{\mathcal{N}}^*(\eta_2) - \langle \theta_1, \eta_2 \rangle.$$

The moment η -parameterization of a normal is $(\eta = \mu, H = -\Sigma - \mu\mu^\top)$ with its reciprocal function $(\lambda = \eta, \Lambda = -H - \eta\eta^\top)$.

Let $F_{\mathcal{P}}(P) = F_{\mathcal{N}}(0, P)$, $\bar{\theta} = \frac{1}{2}\bar{P}^{-1}$, $\bar{\eta} = \nabla F_{\mathcal{P}}(\bar{\theta})$. Then we have the following proposition which proves that the Fenchel-Young divergences in \mathcal{N} and $\bar{\mathcal{N}}$ (as a submanifold of \mathcal{P}) coincide:

Proposition 4 *We have*

$$\begin{aligned} D_{\text{KL}}[p_{\mu_1, \Sigma_1} : p_{\mu_2, \Sigma_2}] &= B_{F_{\mathcal{N}}}(\theta_2 : \theta_1) = Y_{F_{\mathcal{N}}}(\theta_2 : \eta_1) = Y_{F_{\mathcal{P}}}(\bar{\theta}_2 : \bar{\eta}_1) \\ &= B_{F_{\mathcal{P}}}(\bar{\theta}_2 : \bar{\theta}_1) = D_{\text{KL}}[p_{0, \bar{P}_1=f(\mu_1, \Sigma_2)} : p_{0, \bar{P}_2=f(\mu_2, \Sigma_2)}]. \end{aligned}$$

Consider now the ∇^e -geodesics and ∇^m -geodesics on \mathcal{N} (linear interpolation with respect to natural and dual moment parameterizations, respectively): $\gamma_{\mathcal{N}}^e(N_1, N_2; t) = (\mu_t^e, \Sigma_t^e)$ and $\gamma_{\mathcal{N}}^m(N_1, N_2; t) = (\mu_t^m, \Sigma_t^m)$.

Proposition 5 (Mixture geodesics preserved) *The mixture geodesics are preserved by the embedding f : $f(\gamma_{\mathcal{N}}^m(N_1, N_2; t)) = \gamma_{\mathcal{P}}^m(f(N_1), f(N_2); t)$. The exponential geodesics are preserved for subspace of \mathcal{N} with fixed mean μ : \mathcal{N}_μ .*

Proof: For the m -geodesics, let us check that

$$f(\mu_t^m, \Sigma_t^m) = \begin{bmatrix} \Sigma_t^m + \mu_t^m \mu_t^{m\top} & \mu_t^m \\ (\mu_t^m)^\top & 1 \end{bmatrix} = t \underbrace{f(\mu_1, \Sigma_1)}_{\bar{P}_1} + (1-t) \underbrace{f(\mu_2, \Sigma_2)}_{\bar{P}_2},$$

since $\Sigma_t^m + \mu_t \mu_t^{m\top} = \bar{\Sigma}_t + t\mu_1\mu_1^\top + (1-t)\mu_2\mu_2^\top = t(\Sigma_1 + \mu_1\mu_1^\top) + (1-t)(\Sigma_2 + \mu_2\mu_2^\top)$. Thus we have $f(\gamma_{\mathcal{N}}^m(N_1, N_2; t)) = \gamma_{\mathcal{P}}^m(\bar{P}_1, \bar{P}_2; t)$. \square

Therefore all algorithms on \mathcal{N} which only require m -geodesics or m -projections [4] by minimizing the right-hand side of the KLD can be implemented by algorithms on \mathcal{P} . See for example, the minimum enclosing ball approximation algorithm called BBC in [70]. Notice that $\bar{\mathcal{N}}_\mu$ (fixed mean normal submanifolds) preserve both mixture and exponential geodesics: The submanifolds $\bar{\mathcal{N}}_\mu$ are said doubly auto-parallel [71].

Remark 9 *In [13] (p. 355), exercises 13.8 and 13.9 ask to prove the equivalence of the following statements for \mathcal{S} a submanifold of \mathcal{M} :*

- \mathcal{S} is an exponential family $\Leftrightarrow \mathcal{S}$ is ∇^1 -autoparallel in \mathcal{M} (exercise 13.8),
- \mathcal{S} is a mixture family $\Leftrightarrow \mathcal{S}$ is ∇^{-1} -autoparallel in \mathcal{M} (exercise 13.9).

Let $\bar{P} = \begin{bmatrix} \Sigma + \mu\mu^\top & \mu \\ \mu^\top & 1 \end{bmatrix}$ (with $|\bar{P}| = |\Sigma|$), $\bar{P}^{-1} = \begin{bmatrix} \Sigma^{-1} & -\Sigma^{-1}\mu \\ -\mu^\top\Sigma^{-1} & 1 + \mu^\top\Sigma^{-1}\mu \end{bmatrix}$, and $y = (x, 1)$. Then we have

$$\begin{aligned} q_{\bar{P}}(y) &= \frac{1}{(2\pi)^{\frac{d+1}{2}} \sqrt{|\bar{P}|}} \exp\left(-\frac{1}{2}y^\top \bar{P}^{-1}y\right), \\ &= \frac{1}{(2\pi)^{\frac{d+1}{2}} \sqrt{|\Sigma|}} \exp\left(-\frac{1}{2}y^\top \bar{P}^{-1}y\right), \\ &= \frac{1}{(2\pi)^{\frac{d+1}{2}} \sqrt{|\Sigma|}} \exp\left([x^\top \ 1] \begin{bmatrix} \Sigma^{-1} & -\Sigma^{-1}\mu \\ -\mu^\top\Sigma^{-1} & 1 + \mu^\top\Sigma^{-1}\mu \end{bmatrix} \begin{bmatrix} x \\ 1 \end{bmatrix}\right). \end{aligned}$$

Thus $\bar{\mathcal{N}} = \{q_{\bar{P}}(x, 1)\}$ is an exponential family. Therefore we deduce that \mathcal{P} is ∇^e -autoparallel in \mathcal{P} . However, $\bar{\mathcal{N}}$ is not a mixture family and thus \mathcal{P} is not ∇^m -autoparallel in \mathcal{P} .

6 Conclusion and discussion

The Fisher-Rao distance between multivariate normals is not known in closed form: It is thus usually approximated by costly geodesic shooting techniques [40, 75, 7] in practice which requires time-consuming computations of the Riemannian exponential map. In this work, we consider an alternative approach of approximating the Fisher-Rao distance by approximating the Riemannian lengths of closed-form curves. In particular, we considered the mixed exponential-mixture curved and the projected symmetric positive-definite matrix geodesic obtained from Calvo & Oller isometric SPD submanifold embedding [14]. We also reported a fast to compute simplex square root of Jeffreys' divergence for the Fisher-Rao distance which beats the upper bound of [87] when normal distributions are not too far from each others. Finally, we shows that not only Calvo & Oller SPD submanifold embedding [14] is isometric, it also preserves the Kullback-Leibler divergence, the Fenchel-Young divergence and the mixture geodesics. Our approximation technique extends to elliptical distributions [15, 19] which generalize multivariate normal distributions. We may also consider the Calvo & Oller metric distance [14] (a lower bound on the Fisher-Rao distance) or the metric distance of the symmetric space [53] (which enjoys asymptotically Fisher-Rao geodesics [35]) which admits closed-form formula. The C&O distance is well-suited for short Fisher-Rao distances while the symmetric space distance is well-tailored for large Fisher-Rao distances. The calculations of these closed-form distances rely on eigenvalues.

Yet another alternative distance is the Hilbert projective distance on the SPD cone [69] which only requires to calculate the minimal and maximal eigenvalues:

$$\rho_H(P_1, P_2) = \log \frac{\lambda_{\max}(P_1^{-1}P_2)}{\lambda_{\min}(P_1^{-1}P_2)}.$$

The dissimilarity is said projective on the SPD cone because $\rho_H(P_1, P_2) = 0$ iff. $P_1 = \lambda P_2$ for some $\lambda > 0$. However, it is a proper metric distance on $\bar{\mathcal{N}}$:

$$\rho_H(N_1, N_2) := \rho_H(\bar{P}_1, \bar{P}_2),$$

since $\bar{P}_1 = \lambda \bar{P}_2$ iff. $\lambda = 1$ (because the array element $P_1[d+1, d+1] = P_2[d+1, d+1] = 1$), i.e., $\bar{P}_1 = \bar{P}_2$ implying $P_1 = P_2$ by the isometric diffeomorphism f .

Additional materials is available online at <https://franknielsen.github.io/FisherRaoMVN>

Acknowledgments. I warmly thank Frédéric Barbaresco (Thales) and Mohammad Emtiyaz Khan (Riken AIP) for fruitful discussions about this work.

Notations

Entities

$N(\mu, \Sigma)$	d -variate normal distribution (mean μ , covariance matrix Σ)
$p_{(\mu, \Sigma)}(x)$	Probability density function of $N(\mu, \Sigma)$
$q_{\Sigma}(y) = p_{(0, \Sigma)}(y)$	Probability density function of $N(0, \Sigma)$

P

Positive-definite matrix

Mappings

$$\bar{P} = f_1(N)$$

Calvo & Oller mapping [14] (1990)

$$\hat{P} = f_{-\frac{1}{d+1},1}(N) = \hat{f}(N)$$

Calvo & Oller mapping [15] (2002) or [53]

Sets

\mathcal{N}

Set of multivariate normal distributions $N(\mu, \Sigma)$ (MVNs)

\mathbb{P}

Symmetric positive-definite matrix cone (SPD matrix cone)

\mathbb{P}_c

Set of SPD matrices with fixed determinant c ($\mathbb{P} = \mathbb{R}_{>0} \times \mathbb{P}_c$)

SSPD, \mathbb{P}_1

Set of SPD matrices with unit determinant

Λ

Parameter space of $N(\mu, \Sigma)$: $\mathbb{R}^d \times \mathbb{P}(d)$

$\mathcal{N}_0, \mathcal{P}$

Set of zero-centered normal distributions $N(0, \Sigma)$

\mathcal{N}_Σ

Set of normal distributions $N(\mu, \Sigma)$ with fixed Σ

\mathcal{N}_μ

Set of normal distributions $N(\mu, \Sigma)$ with fixed μ

$\bar{\mathcal{N}}$

Set of SPD matrices $f(N)$

Riemannian length elements

MVN Fisher

$$ds_{\text{Fisher}, \mathcal{N}}^2 = d\mu^\top \Sigma^{-1} d\mu + \frac{1}{2} \text{tr} \left((\Sigma^{-1} d\Sigma)^2 \right)$$

0-MVN Fisher

$$ds_{\text{Fisher}, \mathcal{N}_0}^2 = \frac{1}{2} \text{tr} \left((\Sigma^{-1} d\Sigma)^2 \right)$$

SPD trace

$$ds_{\beta, \text{trace}}^2 = \beta \text{tr}((P dP)^2) \text{ (when } \beta = \frac{1}{2}, ds_{\text{trace}} = ds_{\text{Fisher}, \mathcal{N}_0})$$

SPD Calvo& Oller metric

$$ds_{\text{CO}}^2 = \frac{1}{2} \left(\frac{d\beta}{\beta} \right)^2 + \beta d\mu^\top \Sigma^{-1} d\mu + \frac{1}{2} \text{tr} \left((\Sigma^{-1} d\Sigma)^2 \right)$$

(with $ds_{\text{CO}} = ds_{\mathcal{P}}(f(\mu, \Sigma))$)

when $\beta = 1$, $ds_{\text{CO}} = ds_{\text{Fisher}, \mathcal{N}}$ in $\bar{\mathcal{N}}$

SPD symmetric space

$$ds_{\text{SS}}^2 = \frac{1}{2} d\mu^\top \Sigma^{-1} d\mu + \text{tr} \left((\Sigma^{-1} d\Sigma)^2 \right) - \frac{1}{2} \text{tr}^2(\Sigma^{-1} d\Sigma)$$

Siegel upper space

$$ds_{\text{SH}}^2(Z) = 2 \text{tr} (Y^{-1} dZ Y^{-1} d\bar{Z}) \text{ (} ds_{\text{SH}}(iY) = 2 ds_{\text{Fisher}, \mathcal{N}_0})$$

Manifolds and submanifolds

\mathcal{M} ($= \mathcal{M}_{\mathcal{N}}$)

Manifold of multivariate normal distributions

$\mathcal{S}_\mu \subset \mathcal{M}$

Submanifold of MVNs with μ prescribed

$\mathcal{S}_\Sigma \subset \mathcal{M}$

Submanifold of MVNs with Σ prescribed

\mathcal{M}_Σ

manifold of \mathcal{N}_Σ (non-embedded in \mathcal{M})

\mathcal{M}_μ

manifold of \mathcal{N}_μ (non-embedded in \mathcal{M})

$\mathcal{S}_{[v], \Sigma}$

Submanifold of MVN set $\{N(\lambda v, \Sigma) : \lambda > 0\}$

\mathcal{P}

manifold of symmetric positive-definite matrices

Distances

$\rho_N(N_1, N_2)$

Fisher-Rao distance between normal distributions N_1 and N_2

$\rho_{\text{SPD}}(P_1, P_2)$

Riemannian SPD distance between P_1 and P_2

$\rho_{\text{CO}}(N_1, N_2)$

Calvo & Oller distance from embedding N to $\bar{P} = f(N)$

$\rho_{\text{SS}}(N_1, N_2)$

Symmetric space distance from embedding N to $\hat{P} = \hat{f}(N)$

$D_{\text{KL}}(N_1, N_2)$

Kullback-Leibler divergence between MVNs N_1 and N_2

$D_J(N_1, N_2)$

Jeffreys divergence between MVNs N_1 and N_2

Geodesics and curves

$\gamma_{\mathcal{N}}^{\text{FR}}(N_1, N_2; t)$	Fisher-Rao geodesic between MVNs N_1 and N_2
$\gamma_{\mathcal{P}}^{\text{FR}}(P_1, P_2; t)$	Fisher-Rao geodesic between SPD P_1 and P_2
$\gamma_{\mathcal{N}}^e(N_1, N_2; t)$	exponential geodesic between MVNs N_1 and N_2
$\gamma_{\mathcal{N}}^m(N_1, N_2; t)$	mixture geodesic between MVNs N_1 and N_2
$\gamma_{\mathcal{N}}^{\text{CO}}(N_1, N_2; t)$	projection curve (not geodesic) of $\gamma_{\mathcal{P}}(\bar{P}_1, \bar{P}_2; t)$ onto $\bar{\mathcal{N}}$

References

- [1] Sreangsu Acharyya, Arindam Banerjee, and Daniel Boley. Bregman divergences and triangle inequality. In *Proceedings of the 2013 SIAM International Conference on Data Mining*, pages 476–484. SIAM, 2013.
- [2] Masafumi Akahira and Kei Takeuchi. *Non-regular statistical estimation*, volume 107. Springer Science & Business Media, 2012.
- [3] Syed Mumtaz Ali and Samuel D Silvey. A general class of coefficients of divergence of one distribution from another. *Journal of the Royal Statistical Society: Series B (Methodological)*, 28(1):131–142, 1966.
- [4] Shun-ichi Amari. *Information Geometry and Its Applications*. Applied Mathematical Sciences. Springer Japan, 2016.
- [5] Marc Arnaudon and Frank Nielsen. On approximating the Riemannian 1-center. *Computational Geometry*, 46(1):93–104, 2013.
- [6] Colin Atkinson and Ann FS Mitchell. Rao’s distance measure. *Sankhyā: The Indian Journal of Statistics, Series A*, pages 345–365, 1981.
- [7] Frédéric Barbaresco. Souriau exponential map algorithm for machine learning on matrix Lie groups. In *Geometric Science of Information: 4th International Conference, GSI 2019, Toulouse, France, August 27–29, 2019, Proceedings 4*, pages 85–95. Springer, 2019.
- [8] Martin Bauer, Martins Bruveris, and Peter W Michor. Uniqueness of the fisher-rao metric on the space of smooth densities. *Bulletin of the London Mathematical Society*, 48(3):499–506, 2016.
- [9] Maia Berkane, Kevin Oden, and Peter M Bentler. Geodesic estimation in elliptical distributions. *Journal of Multivariate Analysis*, 63(1):35–46, 1997.
- [10] Martin R Bridson and André Haefliger. *Metric spaces of non-positive curvature*, volume 319. Springer Science & Business Media, 2013.
- [11] Jacob Burbea. Informative geometry of probability spaces. Technical report, PITTSBURGH UNIV PA CENTER FOR MULTIVARIATE ANALYSIS, 1984.
- [12] Jacob Burbea and Josep Maria Oller i Sala. On Rao distance asymptotic distribution. Technical Report Mathematics Preprint Series No. 67, Universitat de Barcelona, 1989.

- [13] Ovidiu Calin and Constantin Udriște. *Geometric modeling in probability and statistics*, volume 121. Springer, 2014.
- [14] Miquel Calvo and Josep M Oller. A distance between multivariate normal distributions based in an embedding into the Siegel group. *Journal of multivariate analysis*, 35(2):223–242, 1990.
- [15] Miquel Calvo and Josep M Oller. A distance between elliptical distributions based in an embedding into the Siegel group. *Journal of Computational and Applied Mathematics*, 145(2):319–334, 2002.
- [16] Miquel Calvo and Josep Maria Oller. An explicit solution of information geodesic equations for the multivariate normal model. *Statistics & Risk Modeling*, 9(1-2):119–138, 1991.
- [17] Nikolai Nikolaevich Cencov. *Statistical decision rules and optimal inference*. American Mathematical Soc., 2000. 53.
- [18] Simone Regina Ceolin and Edwin R Hancock. Computing gender difference using Fisher-Rao metric from facial surface normals. In *25th SIBGRAPI Conference on Graphics, Patterns and Images*, pages 336–343. IEEE, 2012.
- [19] Xiangbing Chen and Jie Zhou. Multisensor estimation fusion on statistical manifold. *Entropy*, 24(12):1802, 2022.
- [20] Xiangbing Chen, Jie Zhou, and Sanfeng Hu. Upper bounds for Rao distance on the manifold of multivariate elliptical distributions. *Automatica*, 129:109604, 2021.
- [21] Anoop Cherian and Suvrit Sra. Riemannian dictionary learning and sparse coding for positive definite matrices. *IEEE transactions on neural networks and learning systems*, 28(12):2859–2871, 2016.
- [22] Antoine Collas, Florent Bouchard, Guillaume Ginolhac, Arnaud Breloy, Chengfang Ren, and J-P Ovarlez. On the Use of Geodesic Triangles between Gaussian Distributions for Classification Problems. In *IEEE International Conference on Acoustics, Speech and Signal Processing (ICASSP)*, pages 5697–5701. IEEE, 2022.
- [23] Antoine Collas, Arnaud Breloy, Chengfang Ren, Guillaume Ginolhac, and Jean-Philippe Ovarlez. Riemannian optimization for non-centered mixture of scaled Gaussian distributions. *arXiv preprint arXiv:2209.03315*, 2022.
- [24] Imre Csiszár. Information-type measures of difference of probability distributions and indirect observation. *studia scientiarum Mathematicarum Hungarica*, 2:229–318, 1967.
- [25] Jason Davis and Inderjit Dhillon. Differential entropic clustering of multivariate Gaussians. *Advances in Neural Information Processing Systems*, 19, 2006.
- [26] Alberto Dolcetti and Donato Pertici. Differential properties of spaces of symmetric real matrices. *arXiv preprint arXiv:1807.01113*, 2018.
- [27] Alberto Dolcetti and Donato Pertici. Elliptic isometries of the manifold of positive definite real matrices with the trace metric. *Rendiconti del Circolo Matematico di Palermo Series 2*, 70(1):575–592, 2021.

- [28] Morris L Eaton. *Group invariance applications in statistics*. Institute of Mathematical Statistics, 1989.
- [29] Poul Svante Eriksen. *Geodesics connected with the fisher metric on the multivariate normal manifold*. Institute of Electronic Systems, Aalborg University Centre, 1986.
- [30] Marco AN Fernandes and Luiz AB San Martin. Fisher information and α -connections for a class of transformational models. *Differential Geometry and its Applications*, 12(2):165–184, 2000.
- [31] Marco AN Fernandes and Luiz AB San Martin. Geometric proprieties of invariant connections on $SL(n, R)/SO(n)$. *Journal of Geometry and Physics*, 47(2-3):369–377, 2003.
- [32] Wolfgang Förstner and Boudewijn Moonen. A metric for covariance matrices. *Geodesy—the Challenge of the 3rd Millennium*, pages 299–309, 2003.
- [33] Jörg Frauendiener, Carine Jaber, and Christian Klein. Efficient computation of multidimensional theta functions. *Journal of Geometry and Physics*, 141:147–158, 2019.
- [34] Akio Fujiwara. Hommage to Chentsov’s theorem. *Information Geometry*, pages 1–20, 2022.
- [35] Wolfgang Globke and Raul Quiroga-Barranco. Information geometry and asymptotic geodesics on the space of normal distributions. *Information Geometry*, 4(1):131–153, 2021.
- [36] Leonor Godinho and José Natário. An introduction to Riemannian geometry. *With Applications*, 2012.
- [37] Teofilo F Gonzalez. Clustering to minimize the maximum intercluster distance. *Theoretical computer science*, 38:293–306, 1985.
- [38] Marvin HJ Gruber. Some applications of the Rao distance to shrinkage estimators. *Communications in Statistics—Theory and Methods*, 37(2):180–193, 2008.
- [39] Abhishek Halder and Tryphon T Georgiou. Gradient flows in filtering and Fisher-Rao geometry. In *2018 Annual American Control Conference (ACC)*, pages 4281–4286. IEEE, 2018.
- [40] Minyeon Han and Frank C Park. DTI segmentation and fiber tracking using metrics on multivariate normal distributions. *Journal of mathematical imaging and vision*, 49:317–334, 2014.
- [41] Trevor Herntier and Adrian M Peter. Transversality conditions for geodesics on the statistical manifold of multivariate gaussian distributions. *Entropy*, 24(11):1698, 2022.
- [42] Harold Hotelling. Spaces of statistical parameters. *Bull. Amer. Math. Soc*, 36:191, 1930.
- [43] Alston S Householder. Unitary triangularization of a nonsymmetric matrix. *Journal of the ACM (JACM)*, 5(4):339–342, 1958.
- [44] Takuro Imai, Akira Takaesu, and Masato Wakayama. Remarks on geodesics for multivariate normal models. Technical report, Faculty of Mathematics, Kyushu University, 2011.

- [45] Hiroto Inoue. Group theoretical study on geodesics for the elliptical models. In *Geometric Science of Information: Second International Conference, GSI 2015, Palaiseau, France, October 28-30, 2015, Proceedings 2*, pages 605–614. Springer, 2015.
- [46] A. T. James. The variance information manifold and the functions on it. In *Multivariate Analysis-III*, pages 157–169. Elsevier, 1973.
- [47] Sebastian Kurtek and Karthik Bharath. Bayesian sensitivity analysis with the Fisher–Rao metric. *Biometrika*, 102(3):601–616, 2015.
- [48] Alice Le Brigant and Stéphane Puechmorel. Quantization and clustering on Riemannian manifolds with an application to air traffic analysis. *Journal of Multivariate Analysis*, 173:685–703, 2019.
- [49] Léo Legrand and Eric Grivel. Evaluating dissimilarities between two moving-average models: A comparative study between jeffrey’s divergence and rao distance. In *2016 24th European Signal Processing Conference (EUSIPCO)*, pages 205–209. IEEE, 2016.
- [50] Peihua Li, Qilong Wang, Hui Zeng, and Lei Zhang. Local log-Euclidean multivariate Gaussian descriptor and its application to image classification. *IEEE transactions on pattern analysis and machine intelligence*, 39(4):803–817, 2016.
- [51] Tengyuan Liang, Tomaso Poggio, Alexander Rakhlin, and James Stokes. Fisher-Rao metric, geometry, and complexity of neural networks. In *The 22nd international conference on artificial intelligence and statistics*, pages 888–896. PMLR, 2019.
- [52] Zhenhua Lin. Riemannian geometry of symmetric positive definite matrices via Cholesky decomposition. *SIAM Journal on Matrix Analysis and Applications*, 40(4):1353–1370, 2019.
- [53] Miroslav Lovrić, Maung Min-Oo, and Ernst A Ruh. Multivariate normal distributions parametrized as a Riemannian symmetric space. *Journal of Multivariate Analysis*, 74(1):36–48, 2000.
- [54] Prasanta Chandra Mahalanobis. On the generalised distance in statistics. In *Proceedings of the national Institute of Science of India*, volume 12, pages 49–55, 1936.
- [55] Luigi Malagò and Giovanni Pistone. Information geometry of the Gaussian distribution in view of stochastic optimization. In *Proceedings of the ACM Conference on Foundations of Genetic Algorithms XIII*, pages 150–162, 2015.
- [56] Gautier Marti, Sébastien Andler, Frank Nielsen, and Philippe Donnat. Optimal transport vs. Fisher-Rao distance between copulas for clustering multivariate time series. In *2016 IEEE statistical signal processing workshop (SSP)*, pages 1–5. IEEE, 2016.
- [57] Charles A Micchelli and Lyle Noakes. Rao distances. *Journal of Multivariate Analysis*, 92(1):97–115, 2005.
- [58] Henrique K Miyamoto, Fábio CC Meneghetti, and Sueli IR Costa. The Fisher–Rao loss for learning under label noise. *Information Geometry*, pages 1–20, 2022.

- [59] Maher Moakher and Mourad Zéraï. The Riemannian geometry of the space of positive-definite matrices and its application to the regularization of positive-definite matrix-valued data. *Journal of Mathematical Imaging and Vision*, 40(2):171–187, 2011.
- [60] Pierre-Alexandre Murena, Antoine Cornuéjols, and Jean-Louis Dessalles. Opening the parallelogram: Considerations on non-euclidean analogies. In *Case-Based Reasoning Research and Development: 26th International Conference, ICCBR 2018, Stockholm, Sweden, July 9-12, 2018, Proceedings 26*, pages 597–611. Springer, 2018.
- [61] Xuan Son Nguyen. Geomnet: A neural network based on Riemannian geometries of SPD matrix space and Cholesky space for 3d skeleton-based interaction recognition. In *Proceedings of the IEEE/CVF International Conference on Computer Vision*, pages 13379–13389, 2021.
- [62] Frank Nielsen. Cramér-Rao lower bound and information geometry. *Connected at Infinity II: A Selection of Mathematics by Indians*, pages 18–37, 2013.
- [63] Frank Nielsen. On the Jensen–Shannon symmetrization of distances relying on abstract means. *Entropy*, 21(5):485, 2019.
- [64] Frank Nielsen. The Siegel–Klein Disk: Hilbert Geometry of the Siegel Disk Domain. *Entropy*, 22(9):1019, 2020.
- [65] Frank Nielsen and Rajendra Bhatia. *Matrix information geometry*. Springer, 2013.
- [66] Frank Nielsen and Gaëtan Hadjeres. Approximating covering and minimum enclosing balls in hyperbolic geometry. In *Geometric Science of Information: Second International Conference, GSI 2015, Palaiseau, France, October 28-30, 2015, Proceedings 2*, pages 586–594. Springer, 2015.
- [67] Frank Nielsen and Richard Nock. Hyperbolic Voronoi diagrams made easy. In *2010 International Conference on Computational Science and Its Applications*, pages 74–80. IEEE, 2010.
- [68] Frank Nielsen and Kazuki Okamura. A note on the f -divergences between multivariate location-scale families with either prescribed scale matrices or location parameters. *arXiv preprint arXiv:2204.10952*, 2022.
- [69] Frank Nielsen and Ke Sun. Clustering in Hilbert’s projective geometry: The case studies of the probability simplex and the ellipsope of correlation matrices. *Geometric structures of information*, pages 297–331, 2019. arXiv:1704.00454.
- [70] Richard Nock and Frank Nielsen. Fitting the smallest enclosing Bregman ball. In *Machine Learning: ECML 2005: 16th European Conference on Machine Learning, Porto, Portugal, October 3-7, 2005. Proceedings 16*, pages 649–656. Springer, 2005.
- [71] Atsumi Ohara. Doubly autoparallel structure on positive definite matrices and its applications. In *International Conference on Geometric Science of Information*, pages 251–260. Springer, 2019.
- [72] Atsumi Ohara, Nobuhide Suda, and Shun-ichi Amari. Dualistic differential geometry of positive definite matrices and its applications to related problems. *Linear Algebra and its Applications*, 247:31–53, 1996.

- [73] Pil S Park and Anant M Kshirsagar. Distances between normal populations when covariance matrices are unequal. *Communications in Statistics-Theory and Methods*, 23(12):3549–3556, 1994.
- [74] Marine Picot, Francisco Messina, Malik Boudiaf, Fabrice Labeau, Ismail Ben Ayed, and Pablo Piantanida. Adversarial robustness via Fisher-Rao regularization. *IEEE Transactions on Pattern Analysis and Machine Intelligence*, 2022.
- [75] Marion Pilté and Frédéric Barbaresco. Tracking quality monitoring based on information geometry and geodesic shooting. In *2016 17th International Radar Symposium (IRS)*, pages 1–6. IEEE, 2016.
- [76] Julianna Pinele, João E Strapasson, and Sueli IR Costa. The Fisher–Rao distance between multivariate normal distributions: Special cases, bounds and applications. *Entropy*, 22(4):404, 2020.
- [77] Branislav Popović, Marko Janev, Lidija Krstanović, Nikola Simić, and Vlado Delić. Measure of Similarity between GMMs Based on Geometry-Aware Dimensionality Reduction. *Mathematics*, 11(1):175, 2022.
- [78] C Radhakrishna Rao. Information and accuracy attainable in the estimation of statistical parameters. *Bulletin of the Calcutta Mathematical Society*, 37(3):81–91, 1945.
- [79] Martin Rios, Angel Villarroja, and Josep M Oller. Rao distance between multivariate linear normal models and their application to the classification of response curves. *Computational statistics & data analysis*, 13(4):431–445, 1992.
- [80] Salem Said, Lionel Bombrun, and Yannick Berthoumieu. Texture classification using Rao’s distance on the space of covariance matrices. In *Geometric Science of Information: Second International Conference, GSI 2015, Palaiseau, France, October 28-30, 2015, Proceedings 2*, pages 371–378. Springer, 2015.
- [81] Hirohiko Shima. *The geometry of Hessian structures*. World Scientific, 2007.
- [82] Carl Ludwig Siegel. *Symplectic geometry*. Elsevier, 2014. first printed in 1964.
- [83] Lene Theil Skovgaard. A Riemannian geometry of the multivariate normal model. *Scandinavian journal of statistics*, pages 211–223, 1984.
- [84] Alexander Soen and Ke Sun. On the variance of the Fisher information for deep learning. *Advances in Neural Information Processing Systems*, 34:5708–5719, 2021.
- [85] João E Strapasson, Julianna Pinele, and Sueli IR Costa. A totally geodesic submanifold of the multivariate normal distributions and bounds for the Fisher-Rao distance. In *IEEE Information Theory Workshop (ITW)*, pages 61–65. IEEE, 2016.
- [86] João E Strapasson, Julianna Pinele, and Sueli IR Costa. Clustering using the Fisher-Rao distance. In *2016 IEEE Sensor Array and Multichannel Signal Processing Workshop (SAM)*, pages 1–5. IEEE, 2016.

- [87] João E Strapasson, Julianna PS Porto, and Sueli IR Costa. On bounds for the Fisher-Rao distance between multivariate normal distributions. *AIP Conference Proceedings*, 1641(1):313–320, 2015.
- [88] Mengjiao Tang, Yao Rong, Jie Zhou, and X Rong Li. Information geometric approach to multisensor estimation fusion. *IEEE Transactions on Signal Processing*, 67(2):279–292, 2018.
- [89] Malik Tiomoko, Romain Couillet, Eric Moisan, and Steeve Zozor. Improved estimation of the distance between covariance matrices. In *IEEE International Conference on Acoustics, Speech and Signal Processing (ICASSP)*, pages 7445–7449. IEEE, 2019.
- [90] Geert Verdoolaege. A new robust regression method based on minimization of geodesic distances on a probabilistic manifold: Application to power laws. *Entropy*, 17(7):4602–4626, 2015.
- [91] Geert Verdoolaege and Paul Scheunders. On the geometry of multivariate generalized Gaussian models. *Journal of mathematical imaging and vision*, 43:180–193, 2012.
- [92] Qilong Wang, Peihua Li, and Lei Zhang. G2denet: Global gaussian distribution embedding network and its application to visual recognition. In *Proceedings of the IEEE conference on computer vision and pattern recognition*, pages 2730–2739, 2017.
- [93] Wen Wang, Ruiping Wang, Zhiwu Huang, Shiguang Shan, and Xilin Chen. Discriminant analysis on Riemannian manifold of Gaussian distributions for face recognition with image sets. In *Proceedings of the IEEE conference on computer vision and pattern recognition*, pages 2048–2057, 2015.
- [94] Joseph Wells, Mary Cook, Karleigh Pine, and Benjamin D Robinson. Fisher-Rao distance on the covariance cone. *arXiv preprint arXiv:2010.15861*, 2020.
- [95] Emo Welzl. Smallest enclosing disks (balls and ellipsoids). In *New Results and New Trends in Computer Science*, pages 359–370. Springer, 2005.
- [96] Shintaro Yoshizawa and Kunio Tanabe. Dual differential geometry associated with the Kullback-Leibler information on the Gaussian distributions and its 2-parameter deformations. *SUT Journal of Mathematics*, 35(1):113–137, 1999.

A Fisher-Rao distance between normal distributions sharing the same covariance matrix

The Rao distance between $N_1 = N(\mu_1, \Sigma)$ and $N_2 = N(\mu_2, \Sigma)$ has been reported in closed-form [76] (Proposition 3). We shall explain the geometric method with full description as follows: Let (e_1, \dots, e_d) be the standard frame of \mathbb{R}^d (ordered basis): The e_i 's are the unit vectors of the axis x_i 's. Let P be an orthogonal matrix such that $P(\mu_2 - \mu_1) = \|\mu_2 - \mu_1\|_2 e_1$ (i.e., matrix P aligns vector $\mu_2 - \mu_1$ to the first axis x_1). Let $\Delta_{12} = \|\mu_2 - \mu_1\|_2$ be the Euclidean distance between μ_1 and μ_2 . Further factorize matrix $P\Sigma P^\top$ using the LDL decomposition (a variant of the Cholesky decomposition) as $P\Sigma P^\top = LDL^\top$ where L is a lower triangular matrix with all diagonal entries equal to one (lower unitriangular matrix of unit determinant) and D a diagonal matrix. Let

$\sigma_{12} = \sqrt{D_{11}}$. Then we have [76]:

$$\rho_{\Sigma}(\mu_1, \mu_2) = \rho_{\mathcal{N}}(N(\mu_1, \Sigma), N(\mu_2, \Sigma)) = \rho_{\mathcal{N}}(N(0, \sigma), N(\Delta_{12}e_1, \sigma_{12})). \quad (25)$$

Note that the right-hand side term is the Fisher-Rao distance between univariate normal distributions of Eq. 4.

To find matrix P , we proceed as follows: Let $u = \frac{\mu_2 - \mu_1}{\|\mu_2 - \mu_1\|_2}$ be the normalized vector to align on axis x_1 . Let $v = u - e_1$. Consider the Householder reflection matrix [43] $M = I - \frac{2vv^{\top}}{\|v\|_2^2}$, where vv^{\top} is a outer product matrix. Since Householder reflection matrices have determinant -1 , we let P be a copy of M with the last row multiplied by -1 so that we get $\det(P) = 1$. By construction, we have $Pu = \|\mu_2 - \mu_1\|_2 e_1$. We then use the affine-invariance property of the Fisher-Rao distance as follows:

$$\begin{aligned} \rho_{\mathcal{N}}(N(\mu_1, \Sigma), N(\mu_2, \Sigma)) &= \rho_{\mathcal{N}}(N(0, \Sigma), N(\mu_2 - \mu_1, \Sigma)), \\ &= \rho_{\mathcal{N}}(N(0, P\Sigma P^{\top}), N(P(\mu_2 - \mu_1), P\Sigma P^{\top})), \\ &= \rho_{\mathcal{N}}(N(0, P\Sigma P^{\top}), N(\Delta_{12}e_1, P\Sigma P^{\top})), \\ &= \rho_{\mathcal{N}}(N(0, LDL^{\top}), N(\Delta_{12}e_1, LDL^{\top})), \\ &= \rho_{\mathcal{N}}(N(0, D), N(\Delta_{12}e_1, D)). \end{aligned}$$

The last row follows from the fact that $L^{-1}e_1 = e_1$ since L^{-1} is an upper unitriangular matrix, and $L^{\top}(L^{-1})^{\top} = (L^{-1}L)^{\top} = I$. The right-hand side Fisher-Rao distance is computed from Eq. 4.

B Embedding multivariate normal distributions in the Siegel upper space

The Siegel upper space is the space of symmetric complex matrices $Z = X + iY = Z^{\top}$ with imaginary positive-definite matrices $Y \succ 0$ [82, 64] (so-called Riemann matrices [33]):

$$\mathbb{S}\mathbb{H}(d) := \{Z = X + iY : X \in \text{Sym}(d), Y \in \mathcal{P}(d)\}, \quad (26)$$

where $\text{Sym}(d)$ is the space of symmetric real $d \times d$ matrices. $\mathbb{S}\mathbb{H}(1)$ corresponds to the Poincaré upper plane. See Figure 19 for an illustration.

The Siegel infinitesimal square line element is

$$ds_{\mathbb{S}\mathbb{H}}^2(Z) = 2\text{tr}(Y^{-1}dZ Y^{-1}d\bar{Z}). \quad (27)$$

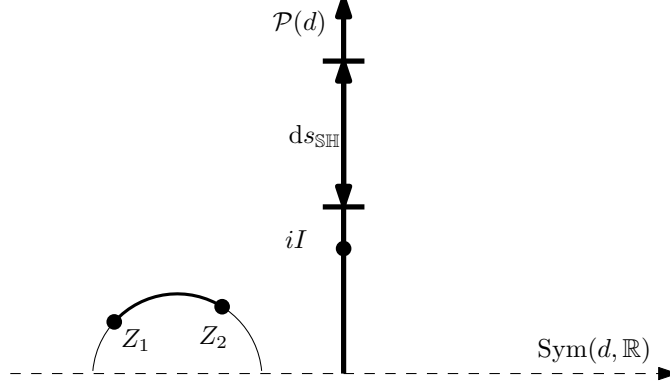
When $X = 0$ and $Z = iY$, we have $dZ = idY$, $d\bar{Z} = -idY$, and it follows that

$$ds_{\mathbb{S}\mathbb{H}}^2(iY) = 2\text{tr}((Y^{-1}dY)^2).$$

That is, four times the square length of the Fisher matrix of centered normal distributions $ds_{\mathcal{N}_0}^2 = \frac{1}{2}\text{tr}((P^{-1}dP)^2)$.

The Siegel distance [82] between Z_1 and $Z_2 \in \mathbb{S}\mathbb{H}(d)$ is

$$\rho_{\mathbb{S}\mathbb{H}}(Z_1, Z_2) = \sqrt{\sum_{i=1}^d \log^2 \left(\frac{1 + \sqrt{r_i}}{1 - \sqrt{r_i}} \right)}, \quad (28)$$



$$ds_{\text{SHH}}(Z) = 2 \operatorname{tr} (Y^{-1} dZ Y^{-1} d\bar{Z})$$

$$\rho_{\text{SHH}}(Z_1, Z_2) = \sqrt{\sum_{i=1}^d \log^2 \left(\frac{1+\sqrt{r_i}}{1-\sqrt{r_i}} \right)}$$

$$r_i = \lambda_i (R(Z_1, Z_2))$$

$$R(Z_1, Z_2) := (Z_1 - Z_2)(Z_1 - \bar{Z}_2)^{-1}(\bar{Z}_1 - \bar{Z}_2)(\bar{Z}_1 - Z_2)^{-1}$$

Figure 19: Siegel upper space generalizes the Poincaré hyperbolic upper plane.

where

$$r_i = \lambda_i (R(Z_1, Z_2)), \quad (29)$$

with $R(Z_1, Z_2)$ denoting the matrix generalization of the cross-ratio

$$R(Z_1, Z_2) := (Z_1 - Z_2)(Z_1 - \bar{Z}_2)^{-1}(\bar{Z}_1 - \bar{Z}_2)(\bar{Z}_1 - Z_2)^{-1}, \quad (30)$$

and $\lambda_i(M)$ denoting the i -th largest (real) eigenvalue of (complex) matrix M . (In practice, we numerically have to round off the tiny imaginary parts to get proper real eigenvalues [64].) The Siegel upper half space is an homogeneous space where the Lie Group $\text{SU}(d, d)/S(U(d) \times U(d))$ acts transitively on it.

We can embed a multivariate normal distribution $N = (\mu, \Sigma)$ into $\text{SHH}(d)$ as follows:

$$N(\mu, \Sigma) \rightarrow Z(N) := \left(\mu\mu^\top + i\Sigma \right),$$

and consider the Siegel distance on the embedded normal distributions as another potential metric distance between multivariate normal distributions:

$$\rho_{\text{SHH}}(N_1, N_2) = \rho_{\text{SHH}}(Z(N_1), Z(N_2)). \quad (31)$$

Notice that the real matrix part of the $Z(N)$'s are all of rank one by construction.